



APPLICATION NO. 09/846,410

TITLE OF INVENTION: Multiple Data Rate Hybrid Walsh Codes for
CDMA

INVENTOR: Urbain A. von der Embse

Clean Copy

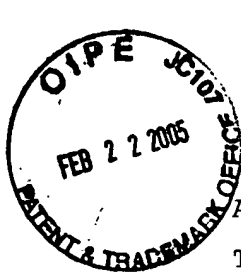


APPLICATION NO. 09/846,410

INVENTOR: Urbain Alfred von der Embse

TITLE OF THE INVENTION

Multiple Data Rate Hybrid Walsh Codes for CDMA



APPLICATION NO. 09/846,410

TITLE OF INVENTION: Multiple Data Rate Hybrid Walsh Codes for
CDMA

INVENTORS: Urbain Alfred von der Embse

CROSS-REFERENCE TO RELATED APPLICATIONS

U.S. PATENT DOCUMENTS

US-6,804,307	Oct 2004	Popović, Branislav SE
US-6,798,737	Sept 2004	Dabak et.al.
US-6,674,712	Jan 2004	Yang et.al.
US-6,396,804	May 2002	Oldenwalder, Joseph P.
US-6,389,138	May 2002	Li et.al.
US-6,185,246	Feb 2002	Gilhousen et.al.
US-2002/0126,741	Sept 2002	Baum et.al.
US-6,317,413	Nov 2001	Honkasalo, Zhi-Chun
US-6,167,079	Dec 2000	Kinnunen et.al.
US-6,157,611	Dec 2000	Shanbhag, Abhijit G.
US-6,088,347	Aug 2000	Minn et.al.
US-5,956,345	Sept 1999	Allpress et.al
US-5,946,344	Aug 1999	Warren et.al.
US-5,943,361	Aug 1999	Gilhousen et.al.
US-5,862,453	Jan 1999	Love et.al.
US-5,805,567	Sept 1998	Ramesh, Nallepalli S.
US-5,715,236	Feb 1998	Gilhousen et.al.
US-5,442,625	Aug 1995	Gitlin et.al.
US-5,311,176	May 1994	Gurney, David P.
US-5,103,459	April 1992	Gilhousen et.al.

U.S. PATENT APPLICATIONS

US-9/826,118 Jan 2001 von der Embse, Urbain A.

OTHER PUBLICATIONS

"Multiple Access for Broadband Networks", IEEE Communications magazine July 2000 Vol. 38 No. 7

"Third Generation Mobile Systems in Europe", IEEE Personal Communications April 1998 Vol. 5 No. 2

"Golay Sequences for DS CDMA Applications", J. Seberry, B.J. Wysocki and T.A. Wysocki, University of Wollongong, NSW 2522, Australia, posted on Internet

"Transmit Diversity in 3G CDMA Systems", R.T. Derryberry, S.D. Gray, D.M. Ionescu, G. Mandyam, B. Raghatham, Nokia Research Center, 6000 Connection Drive, Irving TX 75039, posted on Internet

"Walsh functions and their Applications", K.G. Beauchamp's book, Academic Press 1975

"Discrete Complex Walsh Sequences", J. Edmund Gibbs, Div. of Electrical Science, National Physical Laboratory, Teddington, Middlesex, England, published in 1970 Report

"Application of Walsh Functions to Complex Signals", F.R. Ohnsorg, Systems and Research Div. of Honeywell, Inc. Minneapolis, Minnesota, and Office of Control Theory and Application, NASA Electronics Research Center, Cambridge, Mass., published in NRL Conference, 1970

"The Search for Hadamard Matrices", S.W. Goulomb and L.D. Baumert, Jet Propulsion Lab., Calif. Institute of Tech., published in American Math Monthly, Vol. 70, 1963

"The Z4 linearity of Kerdock, Preparate, Goethals and Related Codes", A.R. Hammons, Jr., P.V. Kumar, A.R. Calderbank, N.J.A. Sloan and P. Sole, IEEE Trans. Inform. Theory, vol. 40, pp.301-319, 1994

"Orthogonal Binary Sequences with Wide Range of Correlation Properties", B.J. Wysocki and T.A. Wysocki, School of Electrical, Computer and Telecommunications Engineering, University of Wollongong, NSW 2522, Australia, posted on the Internet

"Transmit Diversity in 3G CDMA Systems", R.T. Derryberry, S.D. Grey, D.M. Ionescu, G. Mandyam, and B. Raghatham, Nokia Research Center, 6000 Connection Drive, Irving TX 750 75039, posted on the Internet

"Data Modulation for a Direct Sequence Pseudonoise Spread Spectrum Communication System", A.L. Kachelmyer, MIT Lincoln Lab. Project Report IFF-7, 29 Sept. 1981

"Aufbau und Eigenschaften von quasiorthogonalen Codekollektiven", W. Herold and M. Aldinger, Archiv fur Elektronik und Uebertragunsteckhik, vol. 27, Nov.1973, pp. 463-470

APPLICATION NO. 09/846,410

TITLE OF INVENTION: Multiple Date Rate Hybrid Walsh Codes for
CDMA

INVENTOR: Urbain Alfred von der Embse

STATEMENT REGARDING FEDERALLY SPONSORED
RESEARCH OR DEVELOPMENT

Not Applicable.

APPLICATION NO. 09/846,410

TITLE OF INVENTION: Multiple date rate Hybrid Walsh Codes
for CDMA

INVENTOR: Urbain Alfred von der Embse

INCORPORATION-BY-REFERENCE OF MATERIAL
SUBMITTED ON A COMPACT DISC

Not Applicable.

APPLICATION NO. 09/846,410

TITLE OF INVENTION: Multiple Data Rate Hybrid Walsh Codes for
CDMA

INVENTOR: Urbain A. von der Embse

5

BACKGROUND OF THE INVENTION

This is a continuation application from No. 09/826,118
10 filed 01/09/2001.

I. Field of the Invention

The present invention relates to CDMA (Code Division
15 Multiple Access) for wireless cellular WANs (wide area networks),
LANs (local area networks), PANs (personal area networks) with
data rates up to multiple T1 (1.544 Mbps) and higher (>100 Mbps),
and to optical CDMA with data rates in the Gbps and higher
ranges. Applications are mobile, point-to-point and satellite
20 communication networks. More specifically the present invention
relates to novel multiple data rate encoders and fast decoders
for Hybrid Walsh and generalized Hybrid Walsh CDMA codes. These
algorithms and implementations offer substantial improvements
over the current real Walsh orthogonal variable spreading factor
25 (OVSF) CDMA codes for the next generation wideband CDMA (W-CDMA).

II. Description of the Related Art

30 Current art is represented by the work on orthogonal
variable spreading factor (OVSF) real Walsh codes for 3G CDMA2000
and W-CDMA, proposed standards for the fourth generation CDMA
(G4) documented in listed IEEE journals including the IEEE
Journal on selected areas in communications August 2000 Vol. 18

No. 8 "Wideband CDMA" devoted to wideband CDMA including OVSF, and the listed patents.

Current art uses real Walsh orthogonal CDMA channelization codes to generate OVSF codes for multiple data rate users and considers CDMA communications spread over a common frequency band for each of the communication channels. With OVSF the CDMA communications channels for each of the multiple rate users are defined by assigning a unique real Walsh orthogonal spreading code to each user. This real Walsh code has a maximum length of N chips with $N=2^M$ where M is an integer, with shorter lengths of $2, 4, \dots, N/2$ for the higher data rate users. These multiple length real Walsh codes have limited orthogonality properties and occupy the same frequency band. These Walsh encoded user signals are summed and then re-spread over the same frequency band by pseudo-noise (PN) codes, to generate the CDMA communications signal which is modulated and transmitted. The communications link consists of a transmitter, propagation path, and receiver, as well as interfaces and control.

20

Transmitter equations (1) describe a representative real Walsh CDMA encoding for multiple data rate users for the transmitters in FIG. 1A, 1B, 1C, 2A. Multiple code length real Walsh codes are defined in 1 in equations (1). The multiple data rate menu in 2 lists the user group $m=0, 1, 2, \dots, M-1$, data symbol rate R_s , code length, and the number of symbols transmitted over each N-chip reference code length. In this invention disclosure it is assumed the user data symbols have the same symbol data encoding which means the multiple data rate users can be categorized according to their symbol rate.

User data symbols and channelization codes are listed in 3 for the multiple data rate users. Users u_m in group m have their index u_m set equal to the Walsh channelization code vector index in $W_{N(m)}$. Code chip n_m of the user code u_m is equal to $W_{N(m)}(u_m, n_m)$

where $n_m=0,1,2,\dots,N(m)-1$ is the chip index and $N(m)=2^m+1$. User data symbols $Z(u_{m,k_m})$ are indexed by u_{m,k_m} where the index $k_m=0,1,2,\dots,N/N(m)-1$ identifies the data symbols of u_m which are transmitted over the N chip code block. The total number of user data symbols transmitted per N chip block is N .

Current multiple data rate real Walsh CDMA encoding (1)

1 N chip Walsh code block

W_N = Walsh NxN orthogonal code matrix consisting of
 N rows of N chip code vectors
 $= [W_N(c)]$ matrix of row vectors $W_N(c)$
 $= [W_N(c,n)]$ matrix of elements $W_N(c,n)$
 $W_N(c)$ = Walsh code vector c for $c=0,1,\dots,N-1$
 $= [W_N(c,0), W_N(c,1), \dots, W_N(c,N-1)]$
 $= 1xN$ row vector of chips $W_N(c,0), \dots, W_N(c,N-1)$
 $W_N(c,n)$ = Walsh code c chip n
 $= +/- 1$ possible values

2 Multiple data rate menu

Group m	Symbol rate R_s , symbols/second	Code length, chips	Symbols in N -chips
0	$1/2T$	2	$N/2$
1	$1/4T$	4	$N/4$
2	$1/8T$	8	$N/8$
⋮	⋮	⋮	⋮
$M-2$	$2/NT$	$N/2$	2
$M-1$	$1/NT$	N	1

where $1/T$ = chip rate
 T = chip interval

3 User data symbols and channelization codes

User symbol rate groups

$m = 0, 1, \dots, M-1$ index of the user groups

u_m = One of $N(m) = 2^{m+1}$ possible users in group m

5 $N(m)$ = Number of code chips for users in group m
= Number of users allowed in group m
= 2^{m+1}

User data symbols

$Z(u_{m,k_m})$ = User u_m data symbol k_m

10 k_m = Index for the user data symbols over the N chip code block, for a user from group m
= $0, 1, 2, \dots, N/N(m)-1$

User channelization codes

$W_{N(m)}(u_m)$ = Walsh $1 \times 2^{m+1}$ dimensional code vector u_m in the
15 $N(m) \times N(m)$ Walsh code matrix, for user u_m in group m

$W_{N(m)}(u_m, n_m)$ = User u_m code chip $n_m = 0, 1, 2, \dots, N(m)-1$

20 **4 Real Walsh encoding and channel combining**

$Z_n(n)$ = Real Walsh CDMA encoded chip n

$$= \sum_{m=0}^{M-1} \sum_{u_m} Z(u_m, k_m) W_{N(m)}(u_m, n=n_m + k_m N(m))$$

5 PN scrambling

$P_2(n)$ = long PN real code

25 $P_R(n), P_I(n)$ = short PN complex code chip n real,
imaginary components

$$\begin{aligned} Z(n) &= Z_n(n) P_2(n) [P_R(n) + j P_I(n)] \\ &= Z_n(n) \text{sign}\{P_2(n)\} [\text{sign}\{P_R(n)\} + j \text{sign}\{P_I(n)\}] \\ &= \text{CDMA real Walsh CDMA encoded complex chips} \\ &\text{where } j = \sqrt{-1} \end{aligned}$$

Walsh encoding and channel combining in **4** encodes each of the users $\{u_m\}$ and their data symbols $\{Z(u_{m,k_m})\}$ with a Walsh code $W_{N(m)}(u_m)$ drawn from the group m of the $N(m)$ chip channelization codes where u_m is the user code. A time delay of 5 $k_m N(m)$ chips before start of the real Walsh encoding of the data symbol k_m in each of the user channels, is required for implementation of the multiple data rate user real Walsh encoding and for the summation of the encoded data chips over the users. Output of this multiple data rate real Walsh encoding and 10 summation over the multiple data rate users is the set of real Walsh CDMA encoded chips $\{Z_n(n)\}$ over the N chip block.

PN scrambling of the real Walsh CDMA encoded chips in **5** is accomplished by encoding the $\{Z_n(n)\}$ with a long code real PN 15 and a short code complex PN. Output of this real Walsh CDMA encoding followed by the complex PN scrambling are the CDMA encoded chips over the N chip block $\{Z(n)\}$.

Receiver equations **(2)** describe a representative multiple 20 data rate real Walsh CDMA decoding for the receiver in FIG. **3A, 3B, 4A.** In **6** the multiple rate codes are orthogonal with respect to the user codes within a group and also between code groups for all code repetitions over the N chip code block. The PN codes **7** have the useful decoding property that the square of 25 each real code chip is unity which is used in the decoding algorithms **8** that perform the inverse of the signal processing for the encoding in equations **(1)** to recover estimates $\{\hat{Z}(u_{m,k_m})\}$ of the transmitter user symbols $\{Z(u_{m,k_m})\}$ from the received estimates $\{\hat{Z}(n)\}$ of the CDMA real Walsh encoded chips 30 $\{Z(n)\}$.

6 Orthogonality properties of the set of real

5 Walsh {2x2, 4x4, 8x8, ...NxN} matrices

The N(m) x N(m) Walsh code matrices are orthogonal

$$N(m)^{-1} \sum_{n_m} W_{N(m)}(\hat{c}_m, n_m) W_{N(m)}(n_m, c_m) = \delta(\hat{c}_m, c_m)$$

where

10 $c_m, n_m = 0, 1, \dots, N(m)-1$

 $\delta(\hat{c}_m, c_m) = \text{Delta function of } \hat{c}_m \text{ and } c_m$

$= 1, 0 \quad \text{for } \hat{c}_m = c_m, \text{ otherwise}$

The N(m) x N(m) and N(m+p) x N(m+p) Walsh code matrices for

15 all m and p ≥ 0 are orthogonal for a subset of codes {u_m} and {u_{m+p}}

$$N(m)^{-1} \sum_{n_m} W_{N(m)}(u_m, n_m) \bullet W_{N(m+p)}(u_{m+p}, n_{m+p}) = 0 \quad \text{for } k_m = 0, 1, 2, \dots, N/N(m)-1$$

$= 0 \quad \text{for } k_m = 0, 1, 2, \dots, N/N(m)-1$

20 7 PN decoding property for P(n) = P_2(n), P_R(n), P_I(n)

$P(n)P(n) = \text{sign}\{P(n)\} \text{ sign}\{P(n)\} = 1$

8 Decoding algorithm

Received estimates {Ẑ(n)} of the transmitted {Z(n)}

25 $\hat{Z}(u_{m,k_m}) =$

$$(2N)^{-1} \sum_{n_m} \hat{Z}(n) \text{ sign}\{P_2(n)\} [\text{sign}\{P_R(n)\} - j \text{ sign}\{P_I(n)\}] \bullet$$

$\text{sign}\{W_{N(m)}(n = n_m + k_m N(m), u_m)\}$

= Receiver estimate of the transmitted complex

$\text{data symbol } Z(u_{m,k_m})$

FIG. 1A CDMA transmitter block diagram is representative of a current CDMA transmitter for multiple data rate real Walsh CDMA encoding in equations (1). This block diagram becomes a representative implementation of the CDMA transmitter for the 5 multiple data rate Hybrid Walsh and generalized Hybrid Walsh CDMA codes when the current multiple data rate real Walsh CDMA encoding 13 is replaced by the multiple data rate Hybrid Walsh and generalized Hybrid Walsh CDMA encoding. Signal processing starts with the stream of user input data words 9. Frame 10 processor 10 accepts these data words and performs the encoding and frame formatting, and passes the outputs to the symbol encoder 11 which encodes the frame symbols into amplitude and phase coded symbols $\{Z(u_{m,k})\}$ 12. These symbols 12 are the inputs to the current multiple data rate real Walsh CDMA encoding 15 in equations (1). Inputs $\{Z(u_{m,k})\}$ 12 are real Walsh encoded, summed over the users, and scrambled by complex PN in the current multiple date rate real Walsh CDMA encoder 13 to generate the complex output chips $\{Z(n)\}$ 14. This encoding 13 is a representative implementation of equations (1). These output 20 chips $Z(n)$ are waveform modulated 15 to generate the analog complex signal $z(t)$ which is single sideband upconverted, amplified, and transmitted (Tx) by the analog front end of the transmitter 15 as the real waveform $v(t)$ 16 at the carrier frequency f_0 whose amplitude is the real part of the complex 25 envelope of the baseband waveform $z(t)$ multiplied by the carrier frequency and the phase angle ϕ accounts for the phase change from the baseband signal to the transmitted signal.

FIG. 1B is a representative wireless cellular communication 30 network application of the generalized CDMA transmitter in FIG. 1A. FIG. 1B is a schematic layout of part of a CDMA network which depicts cells 101,102,103,104 that partition this portion of the area coverage of the network, depicts one of the users 105 located within a cell with forward and reverse communications

links **106** with the cell-site base station **107**, depicts the base station communication links **108** with the MSC/WSC **109**, and depicts the MSC/WSC communication links with another base station **117**, with another MSC/WSC **116**, and with external elements **110,111,112,113,114,115**. One or more base stations are assigned to each cell or multiple cells or sectors of cells depending on the application. One of the base stations **109** in the network serves as the MSC (mobile switching center) or WSC (wireless switching center) which is the network system controller and switching and routing center that controls all of user timing, synchronization, and traffic in the network and with all external interfaces including other MSC's. External interfaces could include satellite **110**, PSTN (public switched telephone network) **111**, LAN (local area network) **112**, PAN (personal area network) **113**, UWB (ultra-wideband network) **114**, and optical networks **115**. As illustrated in the figure, base station **107** is the nominal cell-site station for cells $i-2$, $i-1$, i , $i+1$ identified as **101,102,102,104**, which means it is intended to service these cells with overlapping coverage from other base stations. The cell topology and coverage depicted in the figure are intended to be illustrative and the actual cells could be overlapping and of differing shapes. Cells can be sub-divided into sectors. Not shown are possible subdivision of the cells into sectors and/or combining the cells into sectors. Each user in a cell or sector communicates with a base station which should be the one with the strongest signal and with available capacity. When mobile users cross over to other cells and/or are near the cell boundary a soft handover scheme is employed for CDMA in which a new cell-site base station is assigned to the user while the old cell-site base station continues to service the user for as long as required by the signal strength.

Fig. **1C** depicts a representative embodiment of the CDMA transmitter signal processing in **13,15** of FIG. **1A** for the forward and reverse CDMA links **106** in FIG. **1B** between the base station

and the users for CDMA2000 and W-CDMA that implements the CDMA coding for real Walsh channelization, synchronization, tracking, and scrambling of the data for transmission. Depicted are the principal signal processing from 13,15 in FIG. 1A that is
5 relevant to this invention disclosure. CDMA2000 and W-CDMA use real Walsh codes 120 for channelization of the data expressed in an OVSF layered format.

FIG. 1C data symbol inputs 12 in FIG. 1A to the transmitter
10 CDMA signal processing are the inphase data symbols R 118 and quadrature data symbols I 119 of the complex data symbols Z(u) from the block interleaving processing in the transmitter in 12 in FIG. 1A. As described previously in equation (1) in greater detail, a real Walsh code 120 ranging in length from N=2 to N=2^M
15 chips spreads and channelizes the data by encoding 121 the inphase and quadrature data symbols with rate R=N codes corresponding to the channel assignments of the data chips. A long PN code 122 encodes the inphase and quadrature real Walsh encoded chips 123. The long PN code 122 is a PN code sequence
20 intended to provide separation of the cells and sectors and to provide protection against multipath. Long PN codes 122 for IST-95/IST-95A use code segments from a 42 bit maximal-length shift register code with code length ($2^{42}-1$). The separation between code segments is sufficient to make them statistically
25 independent. These codes can be converted to complex codes by using the code for the real axis and a delayed version of the code for the quadrature axis whereupon the encoding 123 is replaced by a complex multiply operation similar to the short code complex multiply 126 and in 5 in Equation (1). Different
30 code segments are assigned to different cells or sectors to provide statistical independence between the communications links in different cells or sectors. This long PN code covering of the real Walsh encoded chips is followed by a short complex PN code covering in 124,125,126. Short PN codes are used for scrambling
35 and synchronization of CDMA code chips from the real Walsh

encoding of the data symbols after they are multiplied by a long code. These codes include real and complex valued segments of maximal-length shift register sequences and segments of complex Gold codes which range in length from 256 to 38,400 chips and
5 also are used for user separation and sector separation within a cell. Short PN codes also include Kasami sequences, Kerdock codes, and Golay sequences. This complex PN short code encodes the inphase and quadrature chips with a complex multiply operation **126** as described in **5** in Equation **(1)**. Outputs are
10 inphase and quadrature components of the complex chips which have been rate R=1 phase coded with both the long and short PN codes. Low pass filtering (LPF), summation (Σ) over the Walsh channels for each chip symbol, modulation of the chip symbols to generate a digital waveform, and digital-to-analog (D/A) conversion
15 operations **127** are performed on these encoded inphase and quadrature chip symbols to generate the analog inphase $x(t)$ signal **128** and the quadrature $y(t)$ signal **129** which are the components of the complex signal $z(t)=x(t)+jy(t)$ where $j=\sqrt{-1}$. In equations **(1)** the code summation is equivalently performed by
20 the real Walsh encoding. This complex signal $z(t)$ is single-sideband up-converted to an IF frequency and then up-converted by the RF frequency front end to the RF signal $v(t)$ **133** which is defined in **16** in FIG. **1A**. Single sideband up-conversion of the baseband signal is performed by multiplication of the inphase
25 signal $x(t)$ with the cosine of the carrier frequency f_0 **130** and the quadrature signal $y(t)$ by the sine of the carrier frequency **131** which is a 90 degree phase shifted version of the carrier frequency, and summing **132** to generate the real signal $v(t)$ **133**.

30 FIG. **1C** depicts an embodiment of the current CDMA transmitter art and with current art signal processing changes this figure is representative of other current art CDMA transmitter embodiments for this invention disclosure. Other embodiments of the CDMA transmitter include changes in the

ordering of the signal processing, single channel versus multi-channel real Walsh encoding, summation or combining of the Walsh channels by summation over like chip symbols, analog versus digital signal representation, baseband versus IF frequency CDMA processing, the order and placement in the signal processing thread of the Σ , LPF, and D/A signal processing operations, and the up-conversion processing. The order of the rate R=1 PN multiplies in FIG. 1C can be changed since the covering operations implemented by the multiplies are linear in phase, which means the short PN code complex multiply **124,125,126** in FIG. 1C can occur prior to the long PN code multiply **122,123** and moreover the long PN code can be complex with the real multiply **123** replaced by the equivalent complex multiply **126**.

It should be obvious to anyone skilled in the communications art that this example implementation in FIG. 1A, 1B, 1C clearly defines the fundamental CDMA signal processing relevant to this invention disclosure and it is obvious that this example is representative of the other possible signal processing approaches.

FIG. 2A multiple data rate real Walsh CDMA encoding is a representative implementation algorithm for the multiple data rate real Walsh CDMA encoding **13** in FIG. 1A, **120,121** in FIG. 1C, and in equations **(1)**. Inputs are the complex user data symbols $\{Z(u)\}$ **17**. Encoding of each user by the corresponding Walsh code is described in **18** by the implementation of transferring the sign of each Walsh code chip to the user data symbol followed by a 1-to-N(m) expander $1 \uparrow N(m)$ of each data symbol into an $N(m)=2^m+1$ chip sequence using the sign transfer of the Walsh chips. The sign-expander operation **18** generates the N-chip sequence $Z(u_{m,k_m}) \text{sign}\{W(u_m, (n=n_m+k_mN(m)))\}$ for $n=0,1,\dots,N-1$ for each user $\{u_m\}$. This Walsh encoding serves to spread each user data symbol into an orthogonally encoded chip sequence which is

spread over the CDMA communications frequency band. The Walsh encoded chip sequences for each of the user data symbols are summed over the users **19** followed by PN encoding with the sequence $P_2(n) [P_R(n) + jP_I(n)]$ **20**. Output is the stream of complex multiple data rate real Walsh CDMA encoded chips $\{Z(n)\}$ **21**.

It should be obvious to anyone skilled in the communications art that this example implementation in FIG. **2A** clearly defines the fundamental CDMA signal processing relevant to this invention disclosure and it is obvious that this example is representative of the other possible signal processing approaches.

15 FIG. **3A** CDMA receiver (Rx) block diagram is representative of a current CDMA receiver for multiple data rate real Walsh CDMA decoding in equations **(2)**. This block diagram becomes a representative implementation of the CDMA receiver which implements the multiple data rate Hybrid Walsh and generalized **20** Hybrid Walsh CDMA decoding when the multiple data rate real Walsh CDMA decoding **27** is replaced by the multiple data rate Hybrid Walsh and generalized Hybrid Walsh CDMA decoding.

25 FIG. **3A** signal processing starts with the user transmitted wavefronts incident at the receiver (Rx) antenna **22** for the users $\{u_m\}$. These wavefronts are combined by addition in the antenna to form the receive (Rx) signal $\hat{v}(t)$ at the antenna output **22** where $\hat{v}(t)$ is an estimate of the transmitted signal $v(t)$ **16** in FIG. **1A**, that is received with errors in time Δt , frequency **30** Δf , phase $\Delta\theta$, and with an estimate $\hat{z}(t)$ of the transmitted complex baseband signal $z(t)$ **16** in FIG. **1A**. This received signal $\hat{v}(t)$ is amplified and downconverted by the analog front end **23** and then synchronized and analog-to-digital (A/D) converted **24**. Outputs from the A/D are filtered and chip detected **25** by

the fullband chip detector, to recover estimates $\{\hat{Z}(n)\}$ 26 of the transmitted signal which is the stream of complex CDMA encoded chips $\{Z(n)\}$ 14 in FIG. 1A. CDMA decoder 27 implements the algorithms in equations (2) by stripping off the PN codes 5 and decoding the received CDMA real Walsh orthogonally encoded chips to recover estimates $\{\hat{Z}(u_{m,k_m})\}$ 28 of the transmitted user data symbols $\{Z(u_{m,k_m})\}$ 12 in FIG. 1A. These estimates 28 are processed by the symbol decoder 29 and the frame processor 30 to recover estimates 31 of the transmitted user data 10 words.

Fig. 3B depicts a representative embodiment of the receiver signal processing 27 in FIG. 3A for the forward and reverse CDMA links 106 in FIG. 1B between the base station and the user for 15 CDMA2000 and W-CDMA that implements the CDMA decoding for the long and short codes, the real Walsh codes, and for recovering estimates \hat{R}, \hat{I} 148,149 of the transmitted inphase and quadrature data symbols R 118 and I 119 in FIG. 1C. Depicted are the principal signal processing that is relevant to this 20 invention disclosure. Signal input $\hat{v}(t)$ 134 in FIG. 3B is the received transmitted CDMA signal v(t) 16 in FIG. 1A and 133 in FIG. 1C. The signal is handed over to the inphase mixer which multiplies $\hat{v}(t)$ by the cosine 135 of the carrier frequency f_0 followed by a low pass filtering (LPF) 137 which removes the 25 mixing harmonics, and to the quadrature mixer which multiplies $\hat{v}(t)$ by the sine 136 of the carrier frequency f_0 followed by the LPF 137 to remove the mixing harmonics. These inphase and quadrature mixers followed by the LPF perform a Hilbert transform on v(t) to down-convert the signal at frequency f_0 and to recover 30 estimates \hat{x}, \hat{y} 138,139 of the inphase component x(t) and the quadrature component y(t) of the transmitted complex baseband CDMA signal $z(t)=x(t)+jy(t)$ in 128,129 FIG. 1C. The $\hat{x}(t)$ and

$\hat{y}(t)$ baseband signals are D/A **140** converted and demodulated (demod.) to recover the transmitted inphase and quadrature baseband chip symbols. The complex short PN code cover is removed by a complex multiply **143** with the complex conjugate of
5 the short PN code implemented by using the inphase short code **141** and the negative of the quadrature short code **142** in the complex multiply operation **143**. The long PN code cover is removed by a real multiply **145** with the long code **144**. The de-covered chip symbols are rate $R=1/N$ decoded by the real Walsh decoders **146**
10 using the real Walsh code **147** which implement the real Walsh decoding **36** in FIG. **4A**. Not shown is the rescaling by the multiplicative factor $(1/4N)$. Decoded output symbols are the estimates \hat{R}, \hat{I} **148,149** of the inphase data symbols R and the quadrature data symbols I from the transmitters **12** FIG. **1A** and
15 **118,119** FIG. **1C**.

FIG. **3B** depicts an embodiment of the current CDMA receiver art and with current art signal processing changes this figure is representative of other current art CDMA receiver embodiments for
20 this invention disclosure. Other embodiments of the CDMA receiver include changes in the ordering of the signal processing, analog versus digital signal representation, down-conversion processing, baseband versus IF frequency CDMA processing, order and placement in the signal processing thread of the Σ , LPF, and A/D
25 signal processing operations, and single channel versus multi-channel real Walsh decoding. Code de-covering is implemented as rate $R=N$ code multiply operations which implement the phase subtraction of the code symbols from the chip symbols. The order of the rate $R=N$ code multiplies in FIG. **3** can be changed since
30 the covering operations implemented by the multiplies are linear in phase, which means the short code complex multiply **141,142,143** in FIG. **3B** can occur prior to the long code multiply **144,145** and moreover the long code can be complex with the real multiply **145** replaced by the equivalent complex multiply **143**.

It should be obvious to anyone skilled in the communications art that this example implementation clearly defines the fundamental current CDMA signal processing relevant to this invention disclosure and it is obvious that this example is representative of the other possible signal processing approaches.

FIG. 4A multiple data rate real Walsh CDMA decoding is a representative implementation algorithm for the multiple data rate real Walsh CDMA decoding 27 in FIG. 3A, 144,145 in FIG. 3B, and in equations (2). Inputs are the received estimates of the multiple data rate comple real Walsh CDMA encoded chips $\{\hat{Z}(n)\}$ 32. The PN codes are stripped off from these chips 33 by implementing the decoding algorithms 8 in equations (2). Real Walsh channelization coding is removed in 34 by a pulse compression operation consisting of multiplying each received chip by the numerical sign of the corresponding Walsh chip for the user and summing the products over the $N(m)=2^m+1$ Walsh chips 20 to recover estimates $\{\hat{Z}(u_{m,k_m})\}$ 35 of the user complex data symbols $\{Z(u_{m,k_m})\}$.

It should be obvious to anyone skilled in the communications art that this example implementation clearly defines the fundamental current CDMA signal processing relevant to this invention disclosure and it is obvious that this example is representative of the other possible signal processing approaches.

For cellular applications the transmitter description describes the transmission signal processing applicable to this invention for both the hub and user terminals, and the receiver describes the corresponding receiving signal processing for the hub and user terminals for applicability to this invention.

For optical communications applications the the microwave processing at the front end of both the transmitter and the receiver is replaced by the optical processing which performs the complex modulation for the optical laser transmission in the transmitter and which performs the optical laser receiving function of the microwave processing to recover the complex baseband received signal.

Complex Walsh codes have been proposed during the early work on Walsh bases and codes, based on the even and odd sequency property of the Walsh bases and their correspondence with the even cosine real components and odd sine imaginary components of the DFT (Discrete Fourier Transform). Sequency for the Walsh is the average rate of phase rotations and is the Walsh equivalent of the frequency rotation for the Fourier and DFT bases. Walsh bases are re-ordered Hadamard bases where the ordering corresponds to increasing sequency. Gibbs in the 1970 report "Discrete Complex Walsh Sequences" develops a complex Walsh basis (each basis vector is a complex orthogonal CDMA code) from the real Walsh with the property that similar to the DFT the real part is an even function and the imaginary part is an odd function and takes the values {1,j,-1,-j}. Ohnsorg et. al. in the 1970 report "Application of Walsh Functions to Complex Signals" developed a complex Walsh basis from the real Walsh by generating a complex binary matrix from the Hadamard representation with values {1,j,-1,j} and combining the scaled sum and differences of this matrix to form a complex Walsh matrix of basic vectors which gives this matrix the real even and imaginary odd properties of the DFT. These complex Walsh bases have had no apparent value in signal processing since they were not derived as an isomorphic mapping from the DFT and therefore do not exhibit any of the DFT performance advantages over the real Walsh and moreover do not have simple and fast algorithms

For optical communications applications the the microwave processing at the front end of both the transmitter and the receiver is replaced by the optical processing which performs the complex modulation for the optical laser transmission in the transmitter and which performs the optical laser receiving function of the microwave processing to recover the complex baseband received signal.

Complex Walsh codes have been proposed during the early work on Walsh bases and codes, based on the even and odd sequency property of the Walsh bases and their correspondence with the even cosine real components and odd sine imaginary components of the DFT (Discrete Fourier Transform). Sequency for the Walsh is the average rate of phase rotations and is the Walsh equivalent of the frequency rotation for the Fourier and DFT bases. Walsh bases are re-ordered Hadamard bases where the ordering corresponds to increasing sequency. Gibbs in the 1970 report "Discrete Complex Walsh Sequences" develops a complex Walsh basis (each basis vector is a complex orthogonal CDMA code) from the real Walsh with the property that similar to the DFT the real part is an even function and the imaginary part is an odd function and takes the values {1,j,-1,-j}. Ohnsorg et. al. in the 1970 report "Application of Walsh Functions to Complex Signals" developed a complex Walsh basis from the real Walsh by generating a complex binary matrix from the Hadamard representation with values {1,j.-1.j} and combining the scaled sum and differences of this matrix to form a complex Walsh matrix of basic vectors which gives this matrix the real even and imaginary odd properties of the DFT. These complex Walsh bases have had no apparent value in signal processing since they were not derived as an isomorphic mapping from the DFT and therefore do not exhibit any of the DFT performance advantages over the real Walsh and moreover do not have simple and fast algorithms

for coding and decoding and as a result they have not been used for CDMA communications.

Yang (US 6,674,712) combines real Walsh codes with the
5 quaternary complex-valued Kerdock codes to generate a set of
quasi-orthogonal CDMA codes using the complex multiply operation
126 in FIG. **1C** to combine the real Walsh codes **120**, **121** with the
complex Kerdock codes upon replacing the complex short PN codes
124, **125** with the Kerdock codes, adding a zero to the Kerdock
10 codes of length (2^K-1) to make them 2^M chip codes and using
real Walsh 2^M chip codes, to allow the phase addition of these
codes in the complex multiply **126**. Prior art represented by the
paper by Hannon et. al. (IEEE Trans. Inform. Theory, vol. 40, pp.
301-319, 1994) and other prior publications derived the Kerdock
15 codes with the permutation and construction algorithm in this
patent. Unlike Yang, current CDMA art uses the same 2^M PN code
for all real Walsh channelization codes which keeps the
orthogonality property while providing the desired low
correlation sidelobe properties.

20

Honkasalo (US-6,317,413) develops a method to assign Walsh
codes to variable data rate users for CDMA communications which
is an application of the current OVSF in equations **(1)**, **(2)** and in
FIG. **2B** to the cellular network example in FIG. **1B** for the link
25 **106** between the mobile user **105** and base station **107**. In the
example Tx implementation for the fundamental and supplementary
users, there are $N_4=2^4=16$ channels available at the highest
data rate R supported by the communications link. Each channel
is encoded with a 1×16 chip Walsh code selected from the 16×16
30 Walsh code matrix W_4 . To support R and lower data rates
 $R/2, R/4, R/8, R/16$ and allow several users to occupy each channel,
the user code lengths are extended to $1 \times N_5$, $1 \times N_6$, $1 \times N_7$,
 $1 \times N_8=2^8=256$ chips respectively as shown in equations **(1)**. From
equations **(1)**, **(2)** the code index c for the lowest data rate can
35 be written as the binary word $c=c_0c_1c_2c_3c_4c_5c_6c_7$ where the c_1, \dots, c_8

are the binary coefficients. The first 4 bits $c_0c_1c_2c_3$ are the W_4 code for users at rate R, the first 5 bits $c_0c_1c_2c_3c_4$ are the W_5 code index for users at data rate $R/2$, . . . , and the 8 bit word $c_0c_1c_2c_3c_4c_5c_6c_7$ is the W_8 code index for the lowest data rate $R/16$.
5 This enables the code assignments to be specified by the 4 bit subfield $c_0c_1c_2c_3$ of c for the 16 channels and the last 4 bits $c_4c_5c_6c_7$ for the lower user data rates. Knowing the channel assignment this allows the users within a channel to be specified by the last 4 bits.

10

Prior art in the vol. 27 November 1973 Archive fur Elektronik und Uebertragungsteckhik paper "Aufbau und Eigenschaften von quasiothogonalen Codekollektiven" and in the
15 1981 Lincoln Lab. report IFF-7 introduced the concept of covering (multiplying) the real Walsh encoded data with a real PN code in order to improve the correlation performance with time and frequency offsets. This concept was introduced well in advance of it's use in the late 1980's introduction of CDMA (US
20 5,103,459) wherein the real Walsh encoded data is covered by a real PN code and which covering was later updated using a complex PN code depicted in **124,125,126** FIG. 1C and de-covered in
141,142,143 FIG. 3B.

25

30

35

SUMMARY OF THE INVENTION

The present invention provides a method and system for
5 multiple data rate fast encoding and fast decoding of Hybrid
Walsh codes and generalized Hybrid Walsh codes for use in CDMA
communications as the orthogonal channelization codes to replace
the real Walsh codes. Hybrid Walsh codes generated in this
invention disclosure are complex Walsh codes that have an
10 isomorphic one-to-one correspondence with the discrete Fourier
transform (DFT) codes. Additionally, the encoding (covering) of
the Hybrid Walsh complex code by a complex PN code is a novel
idea introduced in this invention disclosure.

15 Hybrid Walsh codes are the closest possible approximation
to the DFT with orthogonal code vectors taking the values {1+j,
-1+j, -1-j, 1-j} or equivalently the values {1, j, -1, -j} when
the axes are rotated and renormalized and Hybrid Walsh codes
offer performance improvements over real Walsh codes for CDMA
20 communications. Hybrid Walsh codes are derived by separate
lexicographic reordering permutations with increasing sequency of
real Walsh codes for the inphase (real) components and for the
quadrature (imaginary) components.

25 The invention discloses a method and system for the Hybrid
Walsh encoder and decoder to be generalized by combining with
DFT, Hadamard, and other codes using tensor product construction,
direct sum construction, and functional combining. This
construction for generalized Hybrid Walsh codes increase the
30 choices for the code length by allowing the combined use of
Hybrid Walsh codes with lengths 2^M and $4t$ where M and t are
integers, with DFT complex orthogonal codes with lengths N where
N is an integer, with Hadamard codes, and with quasi-orthogonal
PN families of codes including segments of maximal-length shift

register codes, Gold, Kasami, Golay, Kerdock, Preparate,
Goethals, STC, and with other families of codes.

The invention provides a method and system for implementing
5 simultaneous multiple data rate users with variable code sets
assigned to multiple data rate users and with the capability to
be assigned to different sequency spectrums analogous to
frequency division multiplexing (FDM). Additional advantages
compared to OVSF (orthogonal variable spreading factor) are the
10 added performance improvements that will be realized by using the
codes disclosed in this invention in place of the real Walsh
codes and from the greater number of choices for the code lengths
available compared to real Walsh codes.

15 This invention provides a method and system for the fast
and computationally efficient encoding and decoding of the
Hybrid Walsh and generalized Hybrid Walsh code for multiple data
rates. This invention offers a method and system for providing
the current and future applications of real Walsh channelization
20 codes for CDMA with the option of using the Hybrid Walsh and the
generalized Hybrid Walsh codes. An application can simply turn-
off the complex axis components of the Hybrid Walsh codes to
reduce the signal processing to the real Walsh or equivalently
the real Hadamard codes along the inphase and quadrature axes.

25

30

BRIEF DESCRIPTION OF THE DRAWINGS AND THE PERFORMANCE DATA

The above mentioned and other features, objects, design
5 algorithms, and performance advantages of the present invention
will become more apparent from the detailed description set forth
below when taken in conjunction with the drawings and performance
data wherein like reference characters and numerals denote like
elements, and in which:

10

FIG. 1A is a representative CDMA transmitter signal
processing implementation block diagram with emphasis on the
current multiple data rate real Walsh CDMA encoding and on the
signal processing elements addressed by this invention
15 disclosure.

20

FIG. 1B is a schematic CDMA cellular network with the
communications link between a base station and one of the
multiple users.

25

FIG. 1C depicts the transmit real Walsh CDMA encoding
signal processing implementation for the forward and reverse
links between the base station and the multiple data rate users
in the cellular network.

25

FIG. 1D defines the implementation algorithm of this
invention disclosure for generating Hybrid Walsh codes from real
Walsh.

30

FIG. 1E is an embodiment of this invention disclosure for
the transmit CDMA encoding signal processing implementation for
the cellular network using Hybrid Walsh codes in place of real
Walsh codes for the forward and reverse links between the base
station and multiple data rate users.

FIG. 2A is a representative multiple data rate real Walsh CDMA encoding implementation diagram which contains the signal processing elements addressed by this invention disclosure.

FIG. 2B is a representative multiple data rate Hybrid Walsh CDMA encoding implementation diagram which contains the signal processing elements addressed by this invention disclosure.

10

FIG. 3A is a representative CDMA receiver signal processing implementation block diagram with emphasis on the current multiple data rate real Walsh CDMA decoding and on the signal processing elements addressed by this invention disclosure.

15

FIG. 3B is a representative real Walsh CDMA decoding signal processing implementation for the forward and reverse links between the base station and the multiple data rate users in the cellular network.

20

FIG. 3C is an embodiment of of this invention disclosure for the receive CDMA decoding signal processing implementation for the cellular network using Hybrid Walsh codes in place of real Walsh codes for the forward and reverse links between the base station and the mltiple data rate users.

25

FIG. 4A is a representative CDMA decoding implementation diagram for multiple data rate real Walsh CDMA decoding which contains the signal processing elements addressed by this invention disclosure.

30

FIG. 4B is a representative CDMA decoding implementation diagram for multiple data rate Hybrid Walsh CDMA decoding which contains the signal processing elements addressed by this invention disclosure.

FIG. 5A is a representative CDMA encoding implementation diagram which describes the generalized Hybrid Walsh CDMA fast encoding of multiple data rate users and which contains the
5 signal processing elements addressed by this invention disclosure.

FIG. 5B is a representative CDMA encoding implementation diagram which describes the Hybrid Walsh CDMA fast encoding of
10 multiple data rate users and which contains the signal processing elements addressed by this invention disclosure.

FIG. 6A is a representative CDMA decoding implementation diagram which describes the generalized Hybrid Walsh CDMA fast
15 decoding of multiple data rate users and which contains the signal processing elements addressed by this invention disclosure.

FIG. 6B is a representative CDMA decoding implementation diagram which describes the hybrid Hybrid Walsh CDMA fast decoding of multiple data rate users and which contains the signal processing elements addressed by this invention
20 disclosure.

25

DISCLOSURE OF THE INVENTION

The invention provides the algorithms and implementation
30 architectures to support simultaneous multiple data rates or equivalently simultaneous multiple symbol rates using the Hybrid Walsh and generalized Hybrid Walsh orthogonal CDMA codes. In contrast to current art which assigns multiple length real Walsh codes to the multiple data rate users with the shorter codes

assigned to the higher data rate users, the invention uses same chip length codes with the number of codes adjusted as required for the multiple data rate users and has the ability to assign different sequency spectrums to each data rate group of users.

5 This invention supports fast (efficient) encoding and decoding implementations and provides performance improvements with the use of the Hybrid Walsh and generalized Hybrid Walsh codes in place of the real Walsh codes. Hybrid Walsh codes are 4-phase complex orthogonal CDMA codes to replace the current 2-phase real

10 Walsh codes and to provide improvements that include an increase in the carrier-to-noise ratio (CNR) for data symbol recovery in the receiver, lower correlation side-lobes under timing offsets, lower levels of harmonic interference caused by non-linear amplification of multi-carrier CDMA signals, and reduced phase

15 tracking jitter for code tracking to support both acquisition and synchronization. These performance improvements simply reflect the widely known principle that complex CDMA is better than real CDMA. The generalized Hybrid Walsh offers these same improvements together with the flexibility of more choices in the

20 code lengths at the expense of increasing the number of code phases on the unit circle thereby introducing multiplications in the encoding and decoding implementations.

25 1. Hybrid Walsh Encoder and Decoder

The Hybrid Walsh CDMA orthogonal codes have been invented to be the natural extension of the real Walsh codes to the complex domain. These Hybrid Walsh codes in the N-dimensional

30 complex code space C^N are the extension of the 1-to-1 correspondence between the real Walsh codes and the Fourier codes in the N-dimensional real code space R^N , to the 1-to-1 correspondence between the Hybrid Walsh codes and the DFT codes in C^N .

Equations **(3)** define the DFT complex codes in C^N as a function of the real Fourier codes in R^N . These results together with the correspondence between the Hybrid Walsh and the DFT codes will enable the Hybrid Walsh codes in C^N to be derived as a function of the real Walsh codes in R^N in equations **(4)**. The $N \times N$ matrices F, E, W, \tilde{W} are the respective code matrices for the sets of Fourier, DFT, Walsh, Hybrid Walsh codes in R^N , C^N , R^N , C^N and are constructed with the row code vectors $\{F(c)\}$, $\{E(c)\}$, $\{W(c)\}$, $\{\tilde{W}(c)\}$. Each code vector is a $1 \times N$ vector code sequence with component values on the unit circle. Decoding from a matrix viewpoint is the multiplication of the $N \times N$ code matrix with the conjugate transpose of the $N \times N$ code matrix followed by a rescaling. In **401** the real even cosine code vectors $\{C(c)\}$ and odd sine code vectors $\{S(c)\}$ are defined as the real and imaginary components of $\{E(c)\}$ in C^N . The set of Fourier codes in R^N is the N -code subset **402** of these cosine and sine codes which span R^N . This set of Fourier codes can be used to define the DFT codes **403** by applying the DFT spectral foldover property which observes the DFT harmonic vectors for frequencies $f_{NT} = N/2 + \Delta c$ above the half-Nyquist sampling rate $f_{NT} = N/2$ simply foldover such that the DFT harmonic vector for $f_{NT} = N/2 + \Delta c$ is the DFT basis vector for $f_{NT} = N/2 - \Delta c$ to within a fixed sign and fixed phase angle of rotation. and wherein "f" is the frequency and "T" is the discrete sampling interval. From a mathematical viewpoint, the DFT codes in **403** can be equivalently defined by using the trigonometric identities $C(N/2 + \Delta c) = C(N/2 - \Delta c)$ and $S(N/2 + \Delta c) = (-)S(N/2 - \Delta c)$ together with the Fourier codes **403**.

DFT codes in C^N derived from Fourier in R^N (3)

401 DFT codes in C^N

5 $E = \text{DFT NxN orthogonal code matrix consisting of}$
 N rows of N chip code vectors
 $= [E(c)]$ matrix of row vectors $E(c)$
 $= [E(c,n)]$ matrix of elements $E(c,n)$
 $E(c) = C(c) + j S(c) \quad \text{for } c=0,1,\dots,N-1$
10 where
 $C(c) = \text{Even code vectors for } c=0,1,\dots,N-1$
 $= [1, \cos(2\pi c 1/N), \dots, \cos(2\pi c (N-1)/N)]$
 $S(c) = \text{Odd code vectors for } c=0,1,\dots,N-1$
 $= [0, \sin(2\pi c 1/N), \dots, \sin(2\pi c (N-1)/N)]$
15 $E(c,n) = \text{DFT code } c \text{ chip } n$
 $= e^{(j2\pi cn/N)}$
 $= \cos(2\pi cn/N) + j \sin(2\pi cn/N)$

402 Fourier codes in R^N

20 Fourier codes code set are the N codes:
 Even codes { $C(c)$, $c=0,1,2,\dots,N/2$
 Odd codes { $S(c)$, $c=1,2,\dots,N/2-1$

403 DFT codes derived from Fourier codes

25 for $c = 0,1,\dots,N/2$
 $E(c) = C(0) \quad \text{for } c = 0$
 $= C(c) + j S(c) \quad \text{for } c = 1,2,\dots,N/2-1$
 $= C(N/2) \quad \text{for } c = N/2$
30 for $c = N/2+1, \dots, N-1$
 $= N/2 + \Delta c \quad \text{with } \Delta c = 1, \dots, N/2-1$
 $E(c) = C(N/2 - \Delta c) - j S(N/2 - \Delta c)$

Equations (4) derive the Hybrid Walsh codes in C^N as lexicographic reordering permutations of the real Walsh codes in R^N by combining the 1-to-1 correspondence of the real Walsh codes with the Fourier, the 1-to-1 correspondence of the Hybrid Walsh codes with the DFT, and the derivation of the DFT codes in C^N as a function of the Fourier codes in R^N in 403 in equations (3). In equations (4) the even and odd real Walsh codes in 404 are placed in a 1-to-1 correspondence with the cosine and sine Fourier codes in 405 wherein the 1-to-1 correspondence is indicated by the symbol “~” and the correspondence is in lexicographic ordering with increasing sequency and frequency such that “sequency~frequency” meaning that sequency in the real Walsh domain corresponds to frequency in the Fourier domain. In this invention disclosure the Hybrid Walsh is derived as a unique 1-to-1 correspondence between the Hybrid Walsh codes and the DFT in 407. The derivation in 407 starts with the Hybrid Walsh definition in 406. Next, the Hybrid Walsh codes are defined in 20 in 407 by combining 403 in equations (3) with 404, 405, 406.

Hybrid Walsh codes in C^N derived from real Walsh in R^N (4)

25 **404** Even and odd real Walsh codes in R^N

$$\begin{aligned} W_e(u) &= \text{Even Walsh code vector} \\ &= W(2u) \quad \text{for } u=0,1,\dots,N/2-1 \\ W_o(u) &= \text{Odd Walsh code vectors} \\ &= W(2u-1) \quad \text{for } u=1,\dots,N/2 \end{aligned}$$

30 where W_e , W_o are even,odd real Walsh codes

405 Correspondence between real Walsh and Fourier in R^N

$$\begin{aligned} W(0) &\sim C(0) \\ W_e(c) &\sim C(c) \quad \text{for } c = 1,\dots,N/2-1 \\ W_o(c) &\sim S(c) \quad \text{for } c = 1,\dots,N/2-1 \end{aligned}$$

$$W(N-1) \sim C(N/2)$$

406 Hybrid Walsh $\tilde{W}(c) = W(cr) + j W(ci)$ in C^N

5 $cr = cr(c)$
 = lexicographic reordering permutation for the
 real component of the Hybrid Walsh codes

ci = ci(c)
 = lexicographic reordering permutation for the
 imaginary component of the Hybrid Walsh codes

10

407 Correspondence between Hybrid Walsh and DFT in C^H

$$\tilde{W}(c) \sim E(c) \text{ for } c=0,1,2, \dots, N-1$$

Definition of the Hybrid Walsh codes:

15

$$\text{for } c = 0 \\ \tilde{W}(c) = W(0) + jW(0) \sim E(c) = 1$$

$$\text{for } c = 1, 2, \dots, N/2-1 \\ W(cr) = W_e(c) = W(2c) \sim C(c) = \text{Real}\{E(c)\} \\ W(ci) = W_o(c) = W(2c-1) \sim S(c) = \text{Imag}\{E(c)\}$$

20

$$\text{for } c = N/2 \\ \tilde{W}(c) = W(N-1) + j W(N-1) \sim E(c) = C(N/2)$$

25

$$\text{for } c = N/2 + \Delta c, \Delta c = 1, 2, \dots, N/2-1 \\ W(cr) = W(N-1 - 2\Delta c) \sim C(N/2 - \Delta c) = \text{Real}\{E(c)\} \\ W(ci) = W(N-1 - (2\Delta c - 1)) \\ = W(N-2\Delta c) \sim S(N/2 - \Delta c) = (-) \text{Imag}\{E(c)\}$$

30 An equivalent way to derive the complex Hybrid Walsh code vectors in C^N from the real Walsh basis in R^{2N} is to use a sampling technique which is a known method for deriving a complex DFT basis in C^N from a Fourier real basis in R^{2N} .

FIG. 1D summarizes the Hybrid Walsh implementation algorithms derived in equation (4). The real axis (inphase) reordering permutation 168 in FIG. 1D is implemented as an address change $cr=cr(c)$ of the row vectors in W to define the row vectors $W(cr)$ of the real code components of $\tilde{W}(c)$ in lexicographic ordering with increasing sequency 167. Likewise, the imaginary (quadrature) reordering permutation 169 is defined as an address change $ci=ci(c)$ of the row vectors in W to correspond to the row vectors $W(ci)$ of the imaginary code components of $\tilde{W}(c)$ in lexicographic ordering with increasing sequency 167. These reordering permutations define the Hybrid Walsh code vectors $\tilde{W}(c) = W(cr)+jW(ci)$.

FIG. 1E is the upgrade to the cellular network transmit CDMA encoding in FIG. 1B using the Hybrid Walsh channelization codes in place of the real Walsh codes. FIG. 1E depicts a representative embodiment of the transmitter signal processing for the forward and reverse CDMA links 106 in FIG. 1B between the base station and the user for CDMA2000 and W-CDMA. Similar to FIG. 1C the data inputs are the inphase data symbols R 173 and quadrature data symbols I 174. Inphase 175 Hybrid Walsh codes $W(cr)$ are implemented in FIG. 1D 167,168 and in equations (3). Quadrature 176 Hybrid Walsh codes $W(ci)$ are implemented in FIG. 1D 167,169 and in equations (4). A complex multiply 177 encodes the data symbols with the Hybrid Walsh \tilde{W} codes in the encoder using the inphase (real) $W(cr)$ and quadrature (imaginary) $W(ci)$ code components of $\tilde{W}(c) = W(cr)+j W(ci)$ to generate a rate $R=N$ set of Hybrid Walsh encoded data chips for each inphase and quadrature data symbol. Following the Hybrid Walsh encoding the transmit signal processing in 178-to-189 is identical to the corresponding transmit signal processing in 122-to-133 in FIG. 1C.

FIG. 1E depicts an embodiment of the upgrade to the current CDMA transmitter art using the Hybrid Walsh codes in place of the real Walsh codes and with current art signal processing changes this figure is representative of the use of Hybrid Walsh codes in place of the real Walsh codes for other current art CDMA receiver embodiments of this invention disclosure. Other embodiments of the CDMA transmitter include changes in the ordering of the signal processing, single channel versus multi-channel Hybrid Walsh encoding, summation or combining of the Hybrid Walsh channels by summation over like chip symbols, analog versus digital signal representation, baseband versus IF frequency CDMA processing, the order and placement in the signal processing thread of the Σ , LPF, and D/A signal processing operations, and the up-conversion processing. The order of the rate R=1 PN code multiplies in FIG. 1E can be changed since the covering operations implemented by the multiplies are linear in phase, which means the short code complex multiply 180,181,182 in FIG. 1E can occur prior to the long code multiply 178,179 and moreover the long code can be complex with the real multiply 179 replaced by the equivalent complex multiply 182.

FIG. 3C is the upgrade to the cellular network receive CDMA decoding in FIG. 3B using the Hybrid Walsh complex channelization codes in place of the real Walsh codes. FIG. 3C depicts a representative embodiment of the receiver signal processing for the forward and reverse CDMA links 106 in FIG. 1B between the base station and the user for CDMA2000 and W-CDMA that implements the CDMA decoding for the de-covering by the long real code and the short complex code followed by the Hybrid Walsh decoding to recover estimates of the transmitted inphase (real) data symbols R 173 and quadrature (imaginary) data symbols I 174 in FIG. 1E. Depicted are the principal signal processing that is relevant to this invention disclosure. Signal input $\hat{v}(t)$ 190 is the received estimate of the transmitted CDMA

/

signal $v(t)$ **189** in FIG. **1E**. The receive signal recovery in **191-to-201** is identical to the corresponding receive signal processing in **135-to-145** in FIG. **3B**. The de-covered chip symbols are rate $R=1/N$ decoded by the Hybrid Walsh complex decoder **204**
5 using the complex conjugate of the Hybrid Walsh code structured as the inphase Hybrid Walsh code $W(cr)$ **202** and the negative of the quadrature Hybrid Walsh code $W(ci)$ **203** to implement the complex conjugate of the Hybrid Walsh code in the complex multiply and decoding operations. Not shown is the rescaling by
10 the multiplicative factor $(1/4N)$. Decoded output symbols are the inphase data symbol estimates \hat{R} **205** and the quadrature data symbol estimates \hat{I} **206**.

FIG. **3C** depicts an embodiment of the upgrade to the current
15 CDMA receiver art using the Hybrid Walsh code in place of the real Walsh code and with current art signal processing changes this figure is representative of the use of Hybrid Walsh codes in place of the real Walsh codes for other current art CDMA receiver embodiments of this invention disclosure. Other embodiments of
20 the CDMA receiver include changes in the ordering of the signal processing, analog versus digital signal representation, down-conversion processing, baseband versus IF frequency CDMA processing, the order and placement in the signal processing thread of the Σ , LPF, and A/D signal processing operations, and
25 single channel versus multi-channel Hybrid Walsh decoding. The order of the rate $R=1$ PN code multiplies in FIG. **3C** which perform the code de-covering can be changed since the covering operations implemented by the multiplies are linear in phase, which means the short code complex multiply **197,198,199** can
30 occur after to the long code multiply **200,201** and moreover the long code can be complex with the real multiply **201** replaced by the equivalent complex multiply **199**.

2. Generalized Hybrid Walsh Codes

The generalized Hybrid Walsh orthogonal CDMA codes increase the choices for the code length by allowing the combined use of
5 Hybrid Walsh and DFT orthogonal codes using a tensor product construction, direct sum construction, as well as the possibility for more general functional combining including the use of PN codes. Generalized Hybrid Walsh orthogonal CDMA codes increase the flexibility in choosing the code lengths for
10 multiple data rate users at the implementation cost of introducing multiply operations into the CDMA encoding and decoding or degrading the orthogonality property to quasi-orthogonality.

15 Equations **(5)** list construction and examples of the generalized Hybrid Walsh orthogonal CDMA codes using the tensor product with the NxN DFT matrices E_N and Hybrid Walsh matrices \tilde{W}_N and functional combining with direct sums. Low order CDMA code examples **41** illustrate fundamental relationships between the
20 DFT, Hybrid Walsh, and the real Walsh or equivalently Hadamard. Tensor product construction is defined in **42**. CDMA current and developing standards use the prime 2 which generates a code length $N=2^M$ where $M=\text{integer}$. For applications requiring greater flexibility in code length N , additional primes can be used with
25 the tensor product construction. We illustrate this in the examples **43** with the use of prime=3. The use of prime=3 in addition to the prime=2 in the range of $N=8$ to 64 is observed to increase the number of N choices from 4 to 9 at a modest cost penalty of using multiples of the angle increment 30 degrees for
30 prime=3 in addition to the angle increment 90 degrees for prime=2. As noted in **43** there are several choices in the ordering of the tensor product construction and 2 of these choices are used in the construction. In general, the orthogonal code matrices are dependent on the ordering of the tensor product

which means different orderings produce different orthogonal code matrices. Direct sum construction provides greater flexibility in the choice of N without necessarily introducing a multiply penalty. However, the addition of the zero matrix in the construction is generally not desirable for CDMA communications. A functional combining in **44** in equation **(5)** removes these zero matrices at the cost of relaxing the orthogonality property to quasi-orthogonality.

10 Generalized Hybrid Walsh code construction (5)

41 Examples of low-order codes

$$2 \times 2 \quad E_2 = \begin{bmatrix} 1 & 1 \\ 1 & -1 \end{bmatrix}$$

$$= (e^{-j\pi/4} / \sqrt{2}) * \tilde{W}_2$$

$$= H_2 \quad 2 \times 2 \text{ Hadamard}$$

15 = H₂ 2x2 Hadamard

$$3 \times 3 \quad E_3 = \begin{bmatrix} 1 & 1 & 1 \\ 1 & e^{j2\pi/3} & e^{j2\pi/2/3} \\ 1 & e^{j2\pi/2/3} & e^{j2\pi/3} \end{bmatrix}$$

20

$$4 \times 4 \quad \tilde{W}_4 = \begin{bmatrix} 1+j & 1+j & 1+j & 1+j \\ 1+j & -1+j & -1-j & 1-j \\ 1+j & -1-j & 1+j & -1-j \\ 1+j & 1-j & -1-j & -1+j \end{bmatrix}$$

25

$$E_4 = \begin{bmatrix} 1 & 1 & 1 & 1 \\ 1 & j & -1 & -j \\ 1 & -1 & 1 & -1 \\ 1 & -j & -1 & j \end{bmatrix}$$

30

$$= \left(e^{-j\pi/4} / \sqrt{2} \right) \tilde{W}_4$$

42 Tensor product construction for $N = \prod_k N_k$

Code matrix $C_N = NxN$ generalized Hybrid Walsh
orthogonal CDMA code matrix

5 Tensor product construction of C_N

$$C_N = C_0 \prod_{k>0} \otimes C_{N_k}$$

where C_0, C_{N_k} are DFT, Hybrid Walsh code matrices

Tensor product definition

10 A = $N_a \times N_a$ orthogonal code matrix

B = $N_b \times N_b$ orthogonal code matrix

A \otimes B = Tensor product of matrix A and matrix

B

= $N_a N_b \times N_a N_b$ orthogonal code matrix consisting
of the elements $[a_{ik}]$ of matrix A multiplied
by the matrix B

$$= [a_{ik} B]$$

43 Tensor product construction examples for primes

20 $p=2, 3$ and the range of sizes $8 \leq N \leq 64$

$$8 \times 8 \quad C_8 = \tilde{W}_8$$

$$12 \times 12 \quad C_{12} = \tilde{W}_4 \otimes E_3$$

$$C_{12} = E_3 \otimes \tilde{W}_4$$

$$16 \times 16 \quad C_{16} = \tilde{W}_{16}$$

$$18 \times 18 \quad C_{18} = \tilde{W}_2 \otimes E_3 \otimes E_3$$

$$C_{18} = E_3 \otimes E_3 \otimes \tilde{W}_2$$

$$24 \times 24 \quad C_{24} = \tilde{W}_8 \otimes E_3$$

$$C_{24} = E_3 \otimes \tilde{W}_8$$

$$32 \times 32 \quad C_{32} = \tilde{W}_{32}$$

$$\begin{aligned}
36 \times 36 \quad C_{36} &= \tilde{W}_4 \otimes \tilde{W}_3 \otimes \tilde{W}_3 \\
C_{36} &= \tilde{W}_3 \otimes \tilde{W}_3 \otimes \tilde{W}_4 \\
48 \times 48 \quad C_{48} &= \tilde{W}_{16} \otimes \tilde{W}_3 \\
C_{48} &= \tilde{W}_3 \otimes \tilde{W}_{16} \\
5 \quad 64 \times 64 \quad C_{64} &= \tilde{W}_{64}
\end{aligned}$$

44 Generalized Hybrid Walsh quasi-orthogonal code matrices using functional combining with direct sum construction for $N = \sum_k N_k$

Code matrix $C_N = NxN$ generalized Hybrid Walsh quasi-orthogonal Walsh CDMA code matrix using functional combining with direct sum construction of C_N

15

$$C_N = f(C_0, \prod_{k>0} \oplus C_{N_k}, C_P)$$

wherein

A = $N_a \times N_a$ orthogonal code matrix

B = $N_b \times N_b$ orthogonal code matrix

20

$A \oplus B$ = Direct sum of matrix A and matrix B
 $= N_a + N_b \times N_a + N_b$ orthogonal code matrix

25

$$= \begin{bmatrix} A & O_{N_a \times N_b} \\ \hline \cdots & \cdots \\ O_{N_b \times N_a} & B \end{bmatrix}$$

$O_{N_1 \times N_2}$ = $N_1 \times N_2$ zero matrix

$f(A, b)$ = functional combining operator of A, B
= the element-by-element covering of
 A with B for the elements of $A \neq 0$,
= the element-by-element sum of A and
 B for the elements of $A = 0$

5

C_p = NxN pseudo-orthogonal complex code matrix
 whose row code vectors are independent
 strips of PN codes for the real and
 imaginary components

10

3. Multiple Data Rate Hybrid Walsh Encoder and Decoder

15

Transmitter equations **(6)** describe representative Hybrid Walsh CDMA encoding and decoding algorithms for multiple data rate users for implementation in the transmitters in FIG. **1A** and FIG. **1E**. Hybrid Walsh encoding **45,46** assumes the transmitter (Tx) data symbols $Z(u_{m,k_m})$ in **3** in equations **(1)** have already been formatted or equivalently mapped into the data symbol vector $Z(c)$. Hybrid Walsh decoding **47,48** assumes the receiver (Rx) estimates $\hat{Z}(c)$ are de-formatted or equivalently mapped into the estimates $\hat{Z}(u_{m,k_m})$ of the Tx data symbols. Hybrid Walsh encoding for multiple data rate users is defined in **45** as a scalar set of equations and in **46** as an equivalent vector equation. Data inputs for the Hybrid Walsh N-chip block encoding are the $1 \times N$ data vector $Z(c)$ and the encoded output following PN encoding is the $1 \times N$ encoded chip vector $Z(n)$. For the scalar equations the $Z(c), Z(n)$ are considered to be the scalar components or elements of the vectors $Z(c), Z(n)$ respectively and for the vector equations these are considered to be vectors. Multiple data rate Hybrid Walsh decoding is defined

in 47 as a scalar set of equations and in 48 as a vector equation.

5 Hybrid Walsh multiple data rate encoding and decoding (6)

45 Hybrid Walsh CDMA encoding: scalar definition

$$Z(n) = \sum_c Z(c) \tilde{W}(c, n) P_2(n) [P_R(n) + j P_I(n)]$$

= Hybrid Walsh CDMA encoded chip n

10 where

$Z(c)$ = Data symbol c for $c=0, 1, \dots, N-1$

$\tilde{W}(c, n)$ = complex Walsh code c chip n

$$= W(cr, n) + j W(ci, n)$$

$$= (-1)^{[cr_{M-1}n_0 + \sum_{i=1}^{i=M-1} (cr_{M-1-i} + cr_{M-i})n_i]}$$

$$+ j(-1)^{[ci_{M-1}n_0 + \sum_{i=1}^{i=M-1} (ci_{M-1-i} + ci_{M-i})n_i]}$$

$cr = \sum_{i=0}^{i=M-1} cr_i 2^i$ binary representation of cr

$ci = \sum_{i=0}^{i=M-1} ci_i 2^i$ binary representation of ci

$c = \sum_{i=0}^{i=M-1} c_i 2^i$ binary representation of c

$n = \sum_{i=0}^{i=M-1} n_i 2^i$ binary representation of n

20

46 Hybrid Walsh CDMA encoding: vector definition

$$Z(n) = [Z(c) * \tilde{W}] . * P_2 . * [P_R + j P_I]$$

= Hybrid Walsh CDMA encoded chip vector $Z(n)$

where

25 $Z(n) = [Z(n=0), Z(n=1), \dots, Z(n=M-1)]()$

= $1 \times N$ row vector of encoded chips

$$Z(c) = [Z(c=0), Z(c=1), \dots, Z(c=N-1)]$$

$=$ 1xN row vector of data symbols
 $\cdot \cdot \cdot$ = vector and matrix multiplication
 $\cdot \cdot \cdot$ = element-by-element vector and
matrix multiplication

5

47 Hybrid Walsh CDMA decoding: scalar definition

$$\begin{aligned}
\hat{Z}(c) &= (4N)^{-1} \sum_c \hat{Z}(n) \tilde{W}(c,n)' P_2(n) [P_R(n) + j P_I(n)] \\
&= (4N)^{-1} \sum_c \hat{Z}(n) [\text{sign}\{W(n,cr)\} - j \text{sign}\{W(n,ci)\}] \\
&\quad * \text{sign}\{P_2(n)\} [\text{sign}\{P_R(n)\} - j \text{sign}\{P_I(n)\}] \\
&= \text{Receiver estimate of the Tx data symbol } Z(c)
\end{aligned}$$

10

48 Hybrid Walsh CDMA decoding: vector definition

$$\begin{aligned}
\hat{Z}(c) &= (4N)^{-1} [\hat{Z}(n) * \tilde{W}']. * [P_2(n)]. * [P_R(n) + j P_I(n)] \\
&= (4N)^{-1} \hat{Z}(n) * [\text{sign}\{W(n,cr)\} - j \text{sign}\{W(n,ci)\}] \\
&\quad . * [\text{sign}\{P_2(n)\}] . * [\text{sign}\{P_R(n)\} - j \text{sign}\{P_I(n)\}] \\
&= \text{Receiver estimate of the Tx data vector } Z(c)
\end{aligned}$$

20

Equations (7) define a mapping (formatting) of the data input symbol vector for multiple data rate users into the code symbol vector which is constructed by partitioning the code field of elements c into overlapping subfields which can be placed into a 1-to-1 correspondence with the user groups arranged according to data rate. This correspondence together with the arrangement of the partitioning over the field of c codes defines the mapping algorithm for the multiple users and ensures that all users in the same group with the same data symbol rate will occupy the same sequency spectrum. The menu of allowable symbol rates and the corresponding user groups are defined in 2,3 in equation (1). An alternate approach to mapping (formatting) is to directly assign to the data symbol vector the received data

symbols from the users for transmission over the N-chip CDMA encoded block.

In equations (7) the data field mapping is developed by 5 partitioning the code field of elements {c} into subfields with each subfield assigned to the set of users transmitting at the same data symbol rate, and then assigning the users to their appropriate subfield. This will enable the users within the same group to be contiguous in their Hybrid Walsh code 10 assignments and thereby to transmit over the same sequency band. Partitioning of the code field of elements {c} is defined in 15 **49,50,51** based on binary coefficient representations of the code index c as $c=c_1+c_22+\dots+c^{M-1}2^{M-1}$ and as $c=c_0c_1\dots c_{M-2}c_{M-1}$. The finite set of elements indexed on c is a Galois field GF(2^M) of $N=2^M$ elements. The algorithm in **49,50,51** defines the unique 20 partitioning of the GF(2^M) into subfields for the user groups and is summarized in FIG. 2B.

In **49** in equations (7) the mapping of the input data 20 symbols { $Z(u_m, k_m)$ } onto the data symbol vector $Z(c)$ is a linear transformation consisting of a data symbol store plus a multiplexing to define $Z(c)$ and the mapping is defined in **50,51** and in FIG. 2B. In **50** the M subfields of GF(2^M) $c_{M-1}, c_{M-2}c_{M-1}, c_{M-3}c_{M-2}c_{M-1}, \dots$ are mapped onto the data symbol vector with 25 elements indexed on c. The user groups { u_m } are assigned to subfields in **51** such that subfield c_{M-1} can support 2 users $c_{M-1}=0$ and $c_{M-1}=1$ with each assigned $N/2$ code symbols $c=0, 1, \dots, N/2-1$, and $c=N/2, N/2+1, \dots, N-1$ in the N-code block and each transmits at the symbol rate $R_s=1/2T$. Subfield $c_{M-2}c_{M-1}$ can 30 support 4 users $c_{M-2}c_{M-1}=00, 01, 10, 11$ which allows the users in this group u_2 to transmit at the symbol rate $R_s=1/4T$. In this partitioning the subfield elements are the members of the corresponding user groups and the range of the mapping of the subfield onto the field GF(2^M) is the number of symbols in the

user group assigned to this subfield. In 51 the menu is defined for the symbol rate, user group, and partitioning subfield. Assignment of the parsed subfields to the data vector code slots c is flexible within the constraint that the network operator 5 must distribute the subfields over the code slots c so that the mapping is 1-to-1 which means it must be both unique and non-overlapping.

This mapping as well as the direct mapping of the 10 multiple data rate users onto the data vector enables the Hybrid Walsh block code to have the same flexibility in accommodating multiple data rate users as the real Walsh multiple block codes and with the added advantages of a fast transform, simultaneous transmission of the user data symbols, and the flexibility for 15 assignment of users to contiguous sequence subbands. Examples 1 and 2 in 52 and 53 illustrate representative user assignments to the data fields of the data symbol vector.

20 Mapping of data input into the data symbol vector (7)

49 Data field mapping of data inputs into the data vector

$$\{ Z(u_m, k_m) \} \longrightarrow Z(c)$$

is a linear transformation "longrightarrow" implemented as a 25 multiplexing of the stored input data onto the subfields of c and storing of this data in Z(c) over the N-chip Hybrid Walsh code block and where:

{ $Z(u_m, k_m)$ = input data symbols consisting of user
groups { u_m } data symbols { k_m } over the N-chip
CDMA code block defined in 3 in equations (1)
 $Z(c)$ = data symbol vector for multiple data rate
Hybrid Walsh CDMA encoding over N-chip block

50 Mapping of data fields onto data symbol vector $Z(c)$

Binary representation of code index c

$$c = c_0 + c_1 2 + c_2 4 \dots + c_{M-2} N/4 + c_{M-1} N/2$$

5 where $c_0=0,1, c_1=0,1, c_2=0,1 \dots$ are the binary coefficients of c

Digital word

$$c = c_0 c_1 c_2 \bullet \bullet \bullet c_{M-2} c_{M-1}$$

10

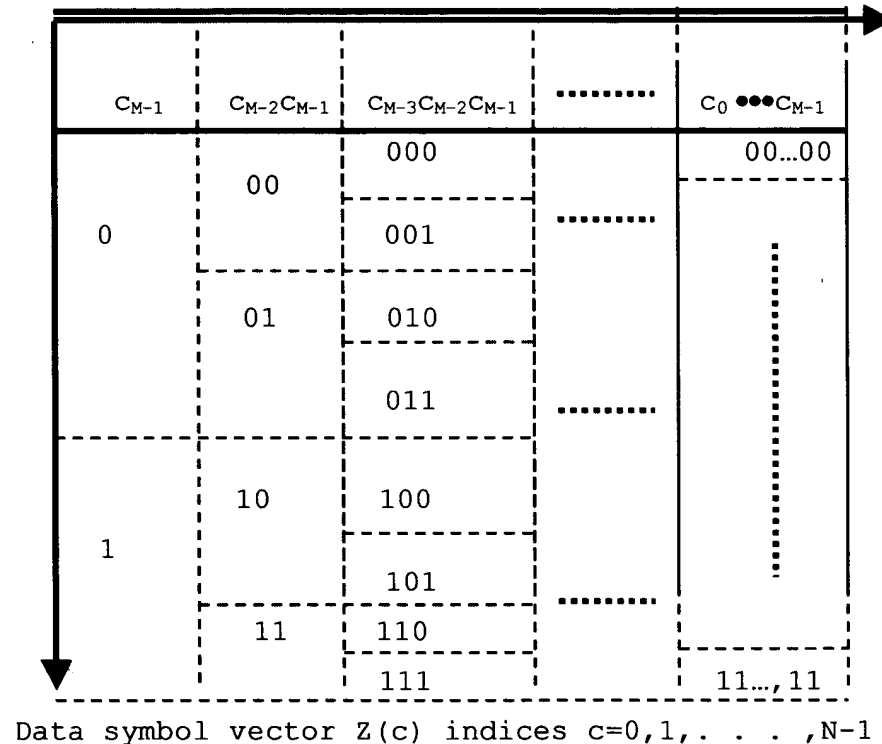
M data fields $c_{M-1}, c_{M-2}c_{M-1}, c_{M-3}c_{M-2}c_{M-1}, \dots, c_0 \bullet \bullet \bullet c_{M-1}$

15

20

25

30



35

51 Menu of user assignment to data vector subfields

	Symbol Rate R_s Symbols/sec.	Users	Data input subfield
5	$1/2T$	$u_0=0$ $=1$	$c_{M-1} = 0$ $=1$
10	$1/4T$	$u_1=0$ $=1$ $=2$ $=3$	$c_{M-2}c_{M-1} = 00$ $=01$ $=10$ $=11$
15	\vdots	\vdots	\vdots
20	$1/NT$	$u_{M-1}=0$ \vdots $=N-1$	$c_0 \bullet \bullet c_{M-1} = 00 \dots 00$ \vdots $=11 \dots 11$

25

30

35

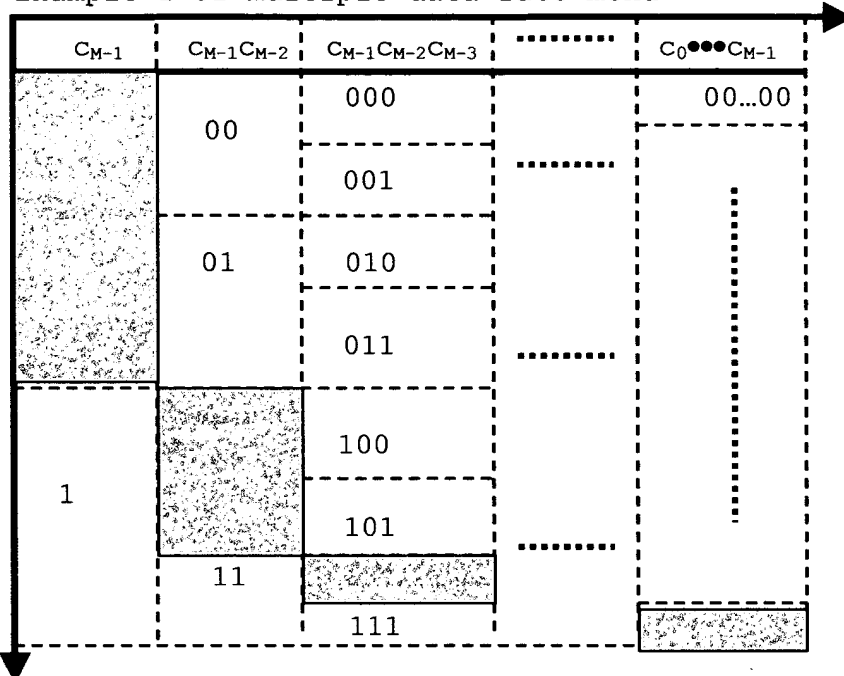
52 Example 1 of multiple data rate menu:

There is 1 user for each group u_0, u_1, \dots, u_{M-2} and 2 users for u_{M-1} with each user selecting the lowest sequence channel corresponding to the lowest index of channels available to the group.

5

Example 1 of multiple data rate menu

10



15

20

25

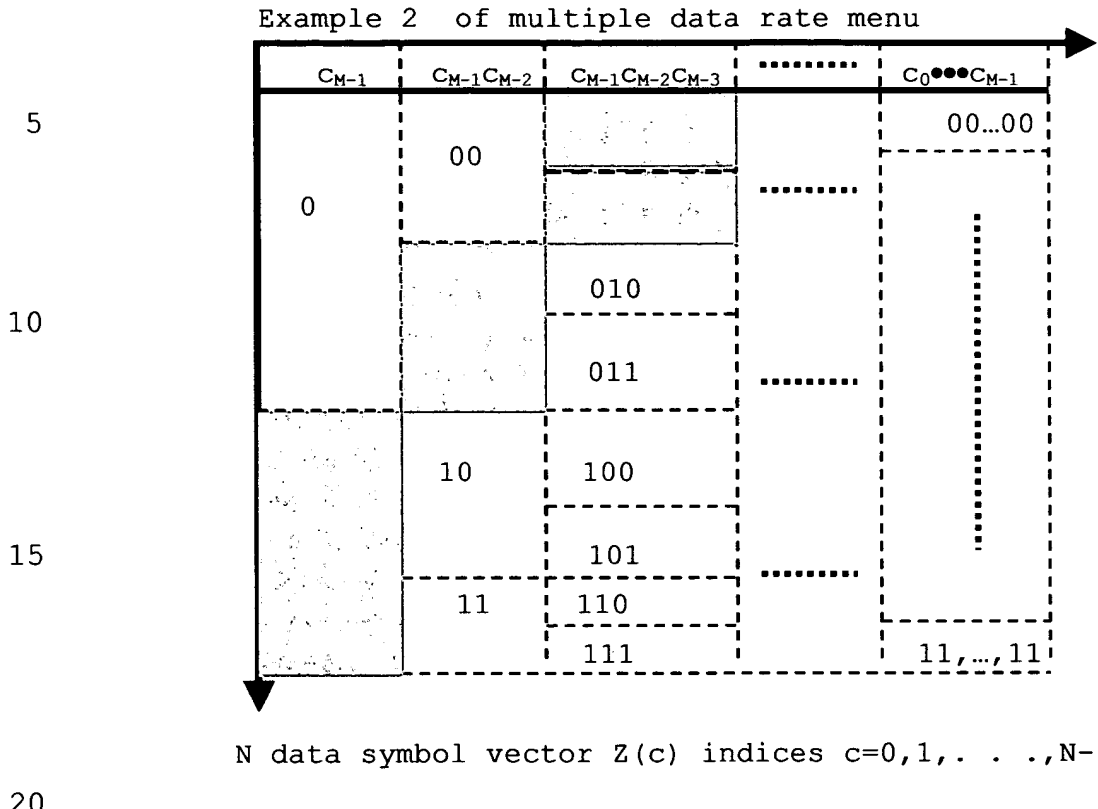
N data symbol vector $Z(c)$ indices $c=0,1,\dots,N-1$

30

53 Example 2 of multiple data rate menu:

There is 1 user in each group u_0 and u_1 and 2 users in u_2 with each user selecting the highest sequence channel corresponding to the highest index of channels available to the group.

35



20

FIG. 2B depicts a representative Tx encoder implementation for the multiple data rate Hybrid Walsh CDMA encoding algorithms in 45,46 in equations (6) using the the data field encoding algorithms in 49-53 in equations (7) as well as the direct mapping algorithms and for application to FIG. 1E for the cellular network and to 1A for general application upon replacing the real Walsh in 13 by the Hybrid Walsh. This encoder maps the received data symbols $\{Z(u_m, k_m)\}$ for the users $\{u_m\}$ onto the data vector $Z(c)$ which is then CDMA encoded over an N -chip block. Input data symbols for each of the users in groups $u_0, u_1, \dots, u_m, \dots, u_{M-1}$ are received 401 and stored 402 in the respective memories $M_0, M_1, \dots, M_m, \dots, M_{M-1}$. The data from these memories is read out and multiplexed (Mux) 403 onto a single

stream of formatted data symbols which define the data symbol vector $Z(c)$ and are stored in memory (Mem) 404. Mux operation is under control of the Mux algorithms 403 which are either the data field algorithms defined in 49-53 in equations (7) or are 5 the direct mapping (formatting) algorithms. The arrows in 403 are "1-to-1" and "onto" mappings. Data symbol vector 405 is read out from Mem and multiplied by the Hybrid Walsh code matrix 406 to generate the Hybrid Walsh encoded vector $Z_n(n)$ 407 which is then covered (encoded) by the long and short PN codes 408 to 10 generate the CDMA encoded chip vector 409.

FIG. 4B depicts a representative Rx decoder implementation for the multiple data rate Hybrid Walsh CDMA decoding algorithms 15 in 47,48 in equations (6) using the inverse of the data field encoding algorithms in 49-53 in equations (7) as well as the inverse of the direct mapping algorithms and for application to FIG. 3C for the cellular network and to 3A for general application upon replacing the real Walsh in 27 by the Hybrid 20 Walsh. Inputs 410 are the Rx estimates $\hat{Z}(n)$ of the Tx CDMA encoded chip vectors $Z(n)$. Long and short PN codes are removed 411 from $\hat{Z}(n)$ by implementing the PN de-covering algorithms 47,48 in equations (6). Next the Hybrid Walsh channelization coding is removed by a matrix multiply operation 412 of the de- 25 covered $\hat{Z}(n)$ with the conjugate transpose \tilde{W}' of the Hybrid Walsh matrix as defined in 47,48 in equations (7). Output is scaled 413 by the multiplicative factor (1/4N) and stored in Mem 414 as the received estimate $\hat{Z}(c)$ of the Tx data symbol vector $Z(c)$. The 30 $\hat{Z}(c)$ is de-multiplexed (de-Mux) by the de-Mux algorithms 416 which are the reversed (inverse) mappings of the data field algorithms and the direct assignment algorithms for the formatting of the data symbol vector. Arrows indicate "1-to-1" and "onto" mappings.

4. Multiple Data Rate Hybrid Walsh Fast Encoder and Fast Decoder

5

Fast encoder and decoder algorithms are computationally efficient algorithms since the number of arithmetic add and multiply operations per data symbol are linear in M where $N=2^M$ for a $N \times N$ Hybrid Walsh code matrix and which is considerably more 10 efficient than the linear dependency on N for direct calculation algorithms. The multiple data rate Hybrid Walsh fast encoder algorithm in equation **(8)** and the fast decoder algorithm in equation **(9)** in this invention disclosure are fast algorithms since their number of real adds per data symbol is approximately 15 $R_A \approx 2M+2$ and the number of real multiplies per data symbol is $R_M=0$.

Hybrid Walsh fast encoder and decoder implementation algorithms are defined in equations **(8)**, **(9)**. The fast encoding algorithm in equations **(8)** implements the encoding of the data 20 symbol vector $Z(c)$ with an M-pass computation of the Hybrid Walsh encoding and a re-ordering pass **54** followed by PN scrambling **55**. Passes $1, 2, 3, \dots, M$ respectively perform the $2, 4, 8, \dots, N$ chip Hybrid Walsh encoding of the data symbol vector successively starting with the 2 chip encoding in pass 1, the 4 chip encoding in passes 25 $1, 2$, the 8 chip encoding in pass $1, 2, 3$, and the N chip encoding in passes $1, 2, 3, \dots, M$ where $N=2^M$. This algorithm is a fast algorithm since the number of real additions R_A per data symbol approximately equal to $R_A \approx 2M+2$ where $N=2^M$ and there are no multiplies. For the real Walsh encoding a fast algorithm 30 requires $R_A \approx M+1$ real additions per data symbol. This fast algorithm generates the Hybrid Walsh CDMA encoded chips in bit reversed order. A re-ordering pass changes the bit reversed output to the normal output. There are other variations to this

algorithm such as starting with the computation of n_0 and proceeding to pass M to calculate n_{M-1} .

(8)

Hybrid Walsh CDMA fast encoding

5 for multiple data rate users

54 Hybrid Walsh fast encoding

Pass 1: $Z^{(1)}(n_{M-1}c_1 \dots c_{M-1})$

$$= \sum Z(c_0 \dots c_{M-1}) [(-1)^{cr_0 n_{M-1}} + j (-1)^{ci_0 n_{M-1}}]$$

\uparrow
 $c_0 = cr_0 = ci_0 = 0, 1$

⋮

Pass m for $m=2, \dots, M-1$

$$Z^{(m)}(n_{M-1} \dots n_{M-m} c_m \dots c_{M-1})$$

$$= \sum Z^{(m-1)}(n_{M-1} \dots n_{M-m+1} c_{m-1} \dots c_{M-1}) \cdot$$

\uparrow
 $[(-1)^{cr_{m-1}(n_{M-m} + n_{M-m+1})} + j (-1)^{ci_{m-1}(n_{M-m} + n_{M-m+1})}]$

$c_{m-1} = cr_{m-1} = ci_{m-1} = 0, 1$

⋮

Pass M: $Z^{(M)}(n_{M-1} n_{M-2} \dots n_1 n_0)$

$$= \sum Z^{(M-1)}(n_{M-1} n_{M-2} \dots n_1 d_{M-1}) \cdot$$

\uparrow
 $[(-1)^{cr_{M-1}(n_0 + n_1)} + j (-1)^{ci_{M-1}(n_0 + n_1)}]$

$c_{M-1} = cr_{M-1} = ci_{M-1} = 0, 1$

$$= Z_n(n_{M-1} n_{M-2} \dots n_1 n_0)$$

25

Re-ordering pass is added to change $Z_n(n_{M-1} n_{M-2} \dots n_1 n_0)$ in bit reversed order to the normal readout:

$$Z_n(n_0 n_1 \dots n_{M-2} n_{M-1}) = Z_n(n)$$

30

55 PN scrambling

$Z(n) = \text{PN scrambled Hybrid Walsh encoded chips}$

$$= Z_n(n) P_2(n) [P_R(n) + j P_I(n)]$$

$$= Z_n(n) \text{sign}\{P_2(n)\} [\text{sign}\{P_R(n)\} + j \text{sign}\{P_I(n)\}]$$

The fast decoding algorithm in equations **(9)** implements the
5 decoding of the Rx CDMA encoded chip vector $\hat{z}(n)$ starting with
the removal of the PN scrambling **56** to yield the Hybrid Walsh
encoded chip vector $\hat{z}_n(n)$ and followed by an M-pass computation
57 of the Hybrid Walsh decoding and a re-ordering plus rescaling
pass to yield the Rx estimate of the transmitted data symbol
10 vector $\hat{z}(c)$. Passes $1, 2, 3, \dots, M$ respectively perform the
 $2, 4, 8, \dots, N$ chip Hybrid Walsh decoding of the encoded chip vector
successively starting with the 2 chip decoding in pass 1, the 4
chip decoding in passes 1,2, the 8 chip decoding in pass 1,2,3,
and the N chip decoding in passes $1, 2, 3, \dots, M$ where $N=2^M$. Like the
15 fast encoding algorithm in equations **(8)** this fast decoding
algorithm in equations **(9)** is a computationally efficient means
to implement the Hybrid Walsh decoding of each N-chip encoded
vector for multiple data rate users whose lowest data rate
corresponds to the data symbol rate of an N-chip encoded user.
20 The number of real additions R_A per data symbol is approximately
equal to $R_A \approx 2M+2$ in the implementation of this fast algorithm
where $N=2^M$. For the real Walsh decoding a fast algorithm
requires $R_A \approx M+1$ real additions per data symbol. A re-ordering
pass changes the bit reversed output to the normal output. There
25 are other variations to this algorithm such as starting with the
computation of c_0 and proceeding to pass M to calculate c_{M-1} .

Hybrid Walsh CDMA fast decoding

(9)

56 PN removed

$$\begin{aligned}
 \hat{Z}_n(n) &= \text{PN removed from CDMA encoded chips } \hat{Z}(n) \\
 &= \hat{Z}(n) P_2(n) [P_R(n) + j P_I(n)] \\
 5 &= \hat{Z}(n) \text{ sign}\{P_2(n)\} [\text{sign}\{P_R(n)\} + j \text{ sign}\{P_I(n)\}]
 \end{aligned}$$

57 Hybrid Walsh fast decoding

$$\begin{aligned}
 \text{Pass 1: } Z^{(1)}(C_{M-1} n_1 \cdots n_{M-1}) \\
 = \sum_{\substack{n_0=0,1 \\ \vdots}} \hat{Z}_n(n_0 \cdots n_{M-1}) [(-1)^{n_0} cr_{M-1} + j (-1)^{n_0} ci_{M-1}]
 \end{aligned}$$

10

$$\begin{aligned}
 \text{Pass m for } m=2, \dots, M-1 \\
 Z^{(m)}(C_{M-1} \cdots C_{M-m} n_m \cdots n_{M-1}) \\
 = \sum_{\substack{\vdots \\ n_{m-1}=0,1}} Z^{(m-1)}(C_{M-1} \cdots C_{M-m+1} n_{m-1} \cdots n_{M-1}) \cdot \\
 [(-1)^{n_{m-1}} (cr_{M-m} + cr_{M-m+1}) \\
 + j (-1)^{n_{m-1}} (ci_{M-m} + ci_{M-m+1})}
 \end{aligned}$$

15

$$\begin{aligned}
 \text{Pass M: } Z^{(M)}(C_{M-1} C_{M-2} \cdots C_1 C_0) \\
 = \sum_{\substack{\vdots \\ n_{M-1}=0,1}} Z^{(M-1)}(C_{M-1} C_{M-2} \cdots C_1 n_{M-1}) \cdot \\
 [(-1)^{n_{M-1}} (cr_0 + cr_1) \\
 + j (-1)^{n_{M-1}} (ci_0 + ci_1) \\
 = \hat{Z}(C_{M-1} C_{M-2} \cdots C_1 C_0)
 \end{aligned}$$

20

25

Reordering and rescaling pass:

$$\begin{aligned}
 30 \hat{Z}(c) &= \hat{Z}(C_0 C_1 \cdots C_{M-2} C_{M-1}) \\
 &= (1/4N) f[\hat{Z}(C_{M-1} C_{M-2} \cdots C_1 C_0)] \\
 &= (1/4N) f[Z^{(M)}(C_{M-1} C_{M-2} \cdots C_1 C_0)]
 \end{aligned}$$

where $f[\hat{Z}]$, $f[Z^M]$ is the bit reversed value of \hat{Z} , Z^M

FIG. 5B depicts a representative implementation block diagram for the Tx fast encoder algorithm in equations (8) for multiple data rate Hybrid Walsh CDMA encoding and executes the
5 fast encoder algorithm in the encoder implementation in FIG. 2B. Received data symbols 418 are mapped by the Mux algorithm 420 into the data symbol vector $Z(c)$ memory Mem 419. The data symbol vector $Z(c)$ is processed by the Hybrid Walsh fast encoding algorithm in equations (8) by executing M passes 421 starting
10 with pass 1 whose output is the partially processed data vector $Z^{(1)}$ and continuing through pass M with output Z^M which then is reordered in another pass and handed over to the Hybrid Walsh encoded vector $Z_n(n)$ memory Mem 422. This vector 423 is scrambled by the long and short PN codes 424 to generate the
15 CDMA encoded chip vector $Z(n)$ 425.

FIG. 6B depicts a representative implementation block diagram for the Rx fast decoder algorithm in equations (9) for multiple data rate Hybrid Walsh CDMA decoding and executes the
20 fast decoder algorithm in the decoder implementation in FIG. 4B. Inputs 426 are the Rx estimates $\hat{Z}(n)$ of the Tx CDMA encoded chip vectors $Z(n)$. Long and short PN codes are removed 427 from $\hat{Z}(n)$ to yield the Rx estimate $\hat{Z}_n(n)$ 428 of the Tx Hybrid Walsh encoded chips $Z_n(n)$. The $Z_n(n)$ is processed by the Hybrid Walsh fast
25 decoding algorithm in equations (8) by executing M passes 429 starting with pass 1 whose output is the partially processed data vector $Z^{(1)}$ and continuing through pass M with output Z^M which is reordered in another pass and rescaled by multiplying by the factor $(1/4N)$ and handed over to the data symbol vector $\hat{Z}(c)$
30 memory Mem 430. The $\hat{Z}(c)$ is de-Multiplexed 431 by the de-Mux algorithms 432 which are the reversed (inverse) mappings of the data field algorithms and the direct assignment algorithms for the formatting of the data symbol vector, to output the Rx

estimates $\{\hat{Z}(u_{m,k_m})\}$ 433 of the Tx user complex data symbols
 $\{Z(u_{m,k_m})\}$.

It should be obvious to anyone skilled in the
5 communications art that the example implementations in FIG.
5B,6B clearly define the fundamental CDMA signal processing
relevant to this invention disclosure and it is obvious that
these examples are representative of the other possible signal
processing approaches.

10

5. Multiple Data Rate Generalized Hybrid Walsh Fast Encoder and Fast Decoder

15 Fast encoder and decoder algorithms are computationally
efficient algorithms since their arithmetic add and multiply
operations per data symbol are linear in the $\{M_n\}$ where $N_n=2^M_n$
is the size of one of the code matrices indexed on "n" in the
construction of the generalized Hybrid Walsh code matrix and
20 which is considerably more efficient than the linear dependency
on $N=N_0 \cdot \cdot \cdot N_n \cdot \cdot \cdot$ for direct calculation algorithms. The
multiple data rate Hybrid Walsh fast encoder algorithm in
equation **(10)** and the fast decoder algorithm in equation **(11)** in
this invention disclosure are fast algorithms since their number
25 of real adds per data symbol is approximately $R_A \approx 2M+M_1+2$ and the
number of real multiplies per data symbol is $R_M=2M_1$ where M refers
to tensor product of the Hybrid Walsh code matrix and M_1 refers
to the DFT code matrix.

30

Equations **(10)** define the fast algorithm for the Tx
encoding of the multiple data rate generalized Hybrid Walsh CDMA
orthogonal codes for the representative example **58** which

constructs the NxN generalized Hybrid Walsh orthogonal CDMA code matrix $C_N = \tilde{W}_{N_0} \otimes E_{N_1}$ as the tensor product of the $N_0 \times N_0$ Hybrid Walsh \tilde{W}_{N_0} and the $N_1 \times N_1$ complex DFT E_{N_1} , where $N=N_0N_1$. Chip element equations are $C_N(c,n) = \tilde{W}_{N_0}(c\tilde{w},n\tilde{w})E_{N_1}(ce,ne)$ with $c = ce + c\tilde{w}N_1$ and $n = ne + n\tilde{w}N_1$ since C_N is the generalized Hybrid Walsh code matrix with each element of \tilde{W}_{N_0} replaced by the matrix E_{N_1} . The binary representation of c,n in **59** is used in the Mux algorithms that map the multiple data rate user symbols into the data symbol vector $Z(c)$ and also are used in the development of the fast encoding algorithm. These c,n binary representations differ from those in **45** in equations **(6)** in the inclusion of the tensor product in the definitions of c,n . Fast encoding **60** encodes the data symbol vector $Z(c)$ with an $M=M_0M_1$ -pass computation starting with the M_0 -pass computation of the Hybrid Walsh encoding and followed by the M_1 -pass computation of the DFT encoding and followed by a re-ordering pass and then by the long and short code PN scrambling **61**. Similar to the Hybrid Walsh fast encoding algorithm in **54** in equations **(8)**, passes $1,2,3,\dots,M_0$ respectively perform the $2,4,8,\dots,N_0$ chip Hybrid Walsh encoding of the data symbol vector and passes $M_0+1,\dots,M=M_0+M_1$ respectively perform the $2,4,8,\dots,N_1$ chip DFT encoding. This fast algorithm generates the generalized Hybrid Walsh CDMA encoded chips in bit reversed order. A re-ordering pass changes the bit reversed output to the normal output $Z_n(n)$ which is scrambled by the PN codes **61** to yield the CDMA encoded chip vector $Z(n)$. There are other variations to this algorithm such as starting with the computation of n_0 and proceeding to pass M to calculate n_{M-1} .

This fast algorithm is a computationally efficient means to implement the generalized Hybrid Walsh encoding of each N-chip code block for multiple data rate users whose lowest data rate

corresponds to the data symbol rate of an N-chip encoded user since the number of real additions R_A per data symbol is approximately equal to $R_A \approx 2M+M_1+2$ and the number of real multiplies R_M per data symbol is $R_M \approx 2M_1$ in the implementation of 5 this fast algorithm where $N=2^M$. Inclusion of the DFT in the generalized Hybrid Walsh adds some multiplies to the computational complexity with the benefit of increasing the choices for the code length N.

10 The mathematical definition and the implementation of the fast encoding algorithm for this example of the generalized Hybrid Walsh are sufficiently detailed to enable this algorithm and implementation to be applied to generalized Hybrid Walsh CDMA codes by someone skilled in the art of CDMA communications and 15 fast transforms.

20 Generalized Hybrid Walsh fast encoding (10)
for multiple data rate users

58 Example NxN generalized Hybrid Walsh code matrix C_N

$$C_N = \tilde{W}_{N_0} \otimes E_{N_1} \text{ tensor product of } \tilde{W}_{N_0} \text{ and } E_{N_1}$$

= $[C_N(c)]$ matrix of row vectors $C_N(c)$

= $[C_N(c, n)]$ matrix of elements $C_N(c, n)$

where $N = N_0N_1$

$$= 2^M$$

$$M = M_0+M_1$$

$$N_0 = 2^{M_0},$$

$$N_1 = 2^{N_1}$$

$$C_N(c, n) = \tilde{W}_{N_0}(c\tilde{w}, n\tilde{w}) E_{N_1}(ce, ne) \text{ code } c \text{ chip } n$$

$$\text{where } c = ce + c\tilde{w} N_1$$

$$n = ne + n\tilde{w} N_1$$

59 Binary representation of c, n in the matrix C_N

$$\begin{aligned}
 c &= ce_0 + ce_1 2 + \dots + ce_{M_1-1} 2^{M_1-1} \\
 &\quad + \tilde{cw}_{M_1} 2^M + \tilde{cw}_{M_1+1} 2^{M_1+1} + \dots + \tilde{cw}_{M-1} 2^{M-1} \\
 &= ce_0 ce_1 \dots ce_{M_1-1} \tilde{cw}_{M_1} \tilde{cw}_{M_1+1} \dots \tilde{cw}_{M-1} \quad \text{Binary word} \\
 &= c_0 + c_1 2 + \dots + c_{M-1} 2^{M-1} \\
 &= c_0 c_1 \dots c_{M-1} \quad \text{Binary word} \\
 n &= ne_0 + ne_1 2 + \dots + ne_{M_1-1} 2^{M_1-1} \\
 &\quad + \tilde{nw}_{M_1} 2^M + \tilde{nw}_{M_1+1} 2^{M_1+1} + \dots + \tilde{nw}_{M-1} 2^{M-1} \\
 &= ne_0 ne_1 \dots ne_{M_1-1} \tilde{nw}_{M_1} \tilde{nw}_{M_1+1} \dots \tilde{nw}_{M-1} \quad \text{Binary word} \\
 &= n_0 + n_1 2 + \dots + n_{M-1} 2^{M-1} \\
 &= n_0 n_1 \dots n_{M-1} \quad \text{Binary word}
 \end{aligned}$$

5

60 Fast encoding of generalized Hybrid Walsh

Pass 1 for Hybrid Walsh codes

$$\begin{aligned}
 Z^{(1)}(c_0 \dots c_{M_1-1} n_{M_0-1} c_{M_1+1} \dots c_{M-1}) \\
 &= \sum Z(c_0 \dots c_{M-1}) \cdot \\
 &\quad [(-1)^{cr_0} n_{M_0-1} + (-1)^{ci_0} n_{M_0-1}] \\
 &\quad \uparrow \\
 &\quad c_{M_1} = cr_0 = ci_0 = 0, 1
 \end{aligned}$$

10

where the Hybrid Walsh indexing reduces to

$$cr_0 = cr_{M_1} \bmod(M_1)$$

$$ci_0 = ci_{M_1} \bmod(M_1)$$

15

Pass m for $m=2, \dots, M_0-1$ for Hybrid Walsh codes

$$\begin{aligned}
 & Z^{(m)} (c_0 \cdots c_{M_1-1} n_{M_0-1} \cdots n_{M_0-m} c_{M_1+m} \cdots c_{M-1}) \\
 & = \sum Z^{(m-1)} (c_0 \cdots c_{M_1-1} n_{M_0-1} \cdots n_{M_0-m+1} c_{M_1+m-1} \cdots c_{M-1}) \cdot \\
 & \quad [(-1)^{cr_{m-1}} (n_{M_0-m} + n_{M_0-m+1}) + \\
 & \quad \quad + j (-1)^{ci_{m-1}} (n_{M_0-m} + n_{M_0-m+1})] \\
 & c_{M_1+m-1} = cr_{m-1} = ci_{m-1} = 0, 1
 \end{aligned}$$

5

where the Hybrid Walsh indexing reduces to

$$\begin{aligned}
 cr_{m-1} &= cr_{M_1+m-1} \bmod (M_1) \\
 ci_{m-1} &= ci_{M_1+m-1} \bmod (M_1)
 \end{aligned}$$

10

Pass M_0 for Hybrid Walsh codes

$$\begin{aligned}
 & Z^{(M_0)} (c_0 \cdots c_{M_1-1} n_{M_0-1} \cdots n_0) \\
 & = \sum Z^{(M-1)} (c_0 \cdots c_{M_1-1} n_{M_0-1} \cdots n_1 c_{M-1}) \cdot \\
 & \quad [(-1)^{cr_{M_0-1}} (n_0 + n_1) \\
 & \quad \quad + j (-1)^{ci_{M_0-1}} (n_0 + n_1)] \\
 & c_{M-1} = cr_{M_0-1} = ci_{M_0-1} = 0, 1
 \end{aligned}$$

15

where the Hybrid Walsh indexing reduces to

$$\begin{aligned}
 cr_{M_0-1} &= cr_{M-1} \bmod (M_1) \\
 ci_{M_0-1} &= ci_{M-1} \bmod (M_1)
 \end{aligned}$$

Pass $M_0+m = M_0+1, \dots, M_0+M_1-1=M-1$ for DFT codes

$$\begin{aligned}
 & Z^{(M_0+m)} (c_0 \cdots c_{M_1-m-1} n_{M_0+m-1} \cdots n_0) \\
 = & \sum Z^{(M_0+m-1)} (c_0 \cdots c_{M_1-m} n_{M_0+m-2} \cdots n_0) \bullet \\
 & \uparrow \\
 & [e^{-(-j)2\pi c_{M_1-m}(n_{M_0} + n_{M_0+1}^2 + \cdots + n_{M_0+m-1}^2)^{m-1}} / 2^m] \\
 c_{M_1-m} = & 0, 1
 \end{aligned}$$

Pass M for DFT codes

$$\begin{aligned}
 & Z^{(M)}(n_{M-1} \dots n_1 n_0) \\
 &= \sum z^{(M-1)}(c_0 n_{M-2} \dots n_1 n_0) \bullet \\
 &\quad \uparrow \\
 &\quad [e^{-j2\pi c_0(n_{M-0} + n_{M-0+1}^2 + \dots + n_{M-1}^{2^M_0 - 1}) / 2^{M_0}}] \\
 &c_0 = 0, 1 \\
 &= Z_n(n_{M-1} n_{M-2} \dots n_1 n_0)
 \end{aligned}$$

15

Re-ordering pass is added to change $Z_n(n_{M-1}n_{M-2}\dots n_1n_0)$ in bit reversed order to the normal readout:

$$Z_n(n_0 n_1 \cdots n_{M-2} n_{M-1}) = Z_n(n)$$

20

61 PN scrambling

$$\begin{aligned} Z(n) &= \text{PN scrambled Hybrid Walsh encoded chips} \\ &= Z_n(n) P_2(n) [P_R(n) + j P_I(n)] \\ &= Z_n(n) \text{sign}\{P_2(n)\} [\text{sign}\{P_R(n)\} + j \text{sign}\{P_I(n)\}] \end{aligned}$$

25

Equations (11) define the fast algorithm for the Rx decoding of the multiple data rate generalized Hybrid Walsh CDMA orthogonal codes for the representative example 58 in equations (10). This fast decoding algorithm implements the decoding of

the Rx CDMA encoded chip vector $\hat{Z}(n)$ starting with the removal of the PN scrambling **62** to yield the Rx estimate of the generalized Hybrid Walsh encoded chip vector $\hat{z}_n(n)$ and followed by an an $M=M_0M_1$ -pass computation starting with the M_0 -pass
5 computation of the Hybrid Walsh decoding and followed by the M_1 -pass computation of the DFT decoding and followed by a re-ordering and rescaling pass to generate the Rx estimate $\hat{Z}(c)$ of the Tx data symbol vector $Z(c)$. Passes $1, 2, 3, \dots, M_0$ respectively perform the $2, 4, 8, \dots, N_0$ chip Hybrid Walsh decoding and passes
10 $M_0+1, \dots, M=M_1+M_0$ respectively perform the $2, 4, 8, \dots, N_0$ chip DFT decoding. There are other variations to this algorithm such as starting with the computation of c_0 and proceeding to pass M to calculate c_{M-1} .

15 This fast algorithm is a computationally efficient means to implement the generalized Hybrid Walsh decoding of each N -chip code block for multiple data rate users whose lowest data rate corresponds to the data symbol rate of an N -chip encoded user It since the number of real additions R_A per data symbol is
20 approximately equal to $R_A \approx 2M+M_1+2$ and the number of real multiplies R_M per data symbol is $R_M \approx 2M_1$ in the implementation of this fast algorithm where $N=2^M$. Inclusion of the DFT in the generalized Hybrid Walsh adds some multiplies to the computational complexity with the benefit of increasing the
25 choices for the code length N .

The mathematical definition and the implementation of the fast decoding algorithm for this example of the generalized Hybrid Walsh are sufficiently detailed to enable this algorithm
30 and implementation to be applied to generalized Hybrid Walsh CDMA codes by someone skilled in the art of CDMA communications and fast transforms.

Generalized Hybrid Walsh fast decoding (11)
 for multiple data rate users
 5 for example 58 in equations (10)

62 PN de-scrambling

$$\begin{aligned}\hat{z}_n(n) &= \text{PN descrambled CDMA encoded chips } \hat{z}(n) \\ &= \hat{z}(n) P_2(n) [P_R(n) + j P_I(n)] \\ 10 &= \hat{z}(n) \text{ sign}\{P_2(n)\} [\text{sign}\{P_R(n)\} + j \text{ sign}\{P_I(n)\}]\end{aligned}$$

**63 Fast decoding of generalized Hybrid Walsh
 for the example 58 in equations (10)**

15 Pass 1 for Hybrid Walsh codes

$$\begin{aligned}Z^{(1)}(c_{M-1} n_1 n_2 \cdots n_{M-2} n_{M-1}) \\ = \sum \hat{z}_n(n_0 n_1 n_2 \cdots n_{M-2} n_{M-1}) \bullet \\ \uparrow \\ n_0 = 0, 1\end{aligned}$$

20

where the Hybrid Walsh indexing reduces to

$$\begin{aligned}cr_{M_0-1} &= cr_{M-1} \bmod(M_1) \\ ci_{M_0-1} &= ci_{M-1} \bmod(M_1)\end{aligned}$$

25 \vdots

Pass m for $m=2, \dots, M_0-1$ for Hybrid Walsh codes

$$\begin{aligned}Z^{(m)}(c_{M-1} c_{M-2} \cdots c_{M-m} n_m \cdots n_{M-2} n_{M-1}) \\ = \sum Z^{(m-1)}(c_{M-1} c_{M-2} \cdots c_{M-m+1} n_{m-1} \cdots n_{M-2} n_{M-1}) \bullet \\ \uparrow \\ n_{m-1} = 0, 1\end{aligned}$$

where the Hybrid Walsh indexing reduces to

$$cr_{M_0-m} + cr_{M_0-m+1} = [cr_{M-m} + cr_{M-m+1}] \bmod (M_1)$$

$$ci_{M_0-m} + ci_{M_0-m+1} = [ci_{M-m} + ci_{M-m+1}] \bmod (M_1)$$

5

⋮

Pass M_0 for Hybrid Walsh codes

$$10 \quad Z^{(M_0)}(c_{M-1} \cdots c_{M_1} n_{M_0} \cdots n_{M-1})$$

$$= \sum Z^{(M_0)}(c_{M-1} \cdots c_{M_1+1} n_{M_0-1} \cdots n_{M-1})$$

$$\uparrow [(-1)^{n_{M_0-1}} (cr_{M_1} + cr_{M_1+1}) - j (-1)^{n_{M_0-1}} (ci_{M_1} + ci_{M_1+1})]$$

$$n_{M_0-1} = 0, 1$$

15

where the Hybrid Walsh indexing reduces to

$$cr_0 + cr_1 = [cr_{M_1} + cr_{M_1+1}] \bmod (M_1)$$

$$ci_0 + ci_1 = [ci_{M_1} + ci_{M_1+1}] \bmod (M)$$

20

Pass $M_0+m = M_0+1, M_0+2, \dots, M_0+M_1-1 = M-1$ for DFT codes

$$Z^{(M_0+m)}(c_{M-1} \cdots c_{M_1} n_{M_0} \cdots n_{M-m-1} c_{m-1} \cdots c_0)$$

$$= \sum Z^{(M_0+m-1)}(c_{M-1} \cdots c_{M_1} n_{M_0} \cdots n_{M-m} c_{m-2} \cdots c_0)$$

$$\uparrow [e^{j 2\pi 2^n n_{M-m} (c_0 + c_1 2 + \cdots + c_{m-1} 2^{m-1}) / 2^m}]$$

25

$$n_{M-m} = 0, 1$$

⋮

Pass M for DFT codes

$$\begin{aligned}
 5 \quad & Z^{(M)} (c_{M-1} \dots c_0) \\
 & = \sum z^{(M_0 + m-1)} (c_{M-1} \dots c_{M_1} n_{M_0} c_{M_1-2} \dots c_0) \\
 & \quad \uparrow \\
 & \quad [e^{j2\pi j n_{M_0}} (c_0 + c_1 2 + \dots + c_{M_1-1} 2^{M_1-1}) / 2^{M_1}] \\
 & \quad n_{M-m} = 0, 1 \\
 & = \hat{Z} (c_{M-1} c_{M-2} \dots c_1 c_0)
 \end{aligned}$$

10

Reordering and rescaling pass:

$$\begin{aligned}
 15 \quad \hat{Z}(c) &= \hat{Z}(c_0 c_1 \dots c_{M-2} c_{M-1}) \\
 &= (1/4N) f[\hat{Z}(c_{M-1} c_{M-2} \dots c_1 c_0)] \\
 &= (1/4N) f[Z^{(M)}(c_{M-1} c_{M-2} \dots c_1 c_0)]
 \end{aligned}$$

where $f[\hat{Z}]$, $f[Z^{(M)}]$ is the bit reversed value of \hat{Z} , $Z^{(M)}$

FIG. 5A depicts a representative implementation block diagram for the Tx fast encoder algorithm in example 58 in equations (10) for multiple data rate generalized Hybrid Walsh CDMA encoding and replaces the real Walsh encoding 13 in FIG. 1A. Received data symbols 434 are mapped by the Mux algorithm 436 into the data symbol vector $Z(c)$ memory Mem 435. The data symbol vector $Z(c)$ is encoded with an $M=M_0 M_1$ -pass computation starting with the M_0 -pass computation of the Hybrid Walsh encoding 437 and followed by the M_1 -pass computation of the DFT encoding 438 to yield $Z^{(M)}$ which is reordered in another pass and handed over to the encoded vector $Z_n(n)$ memory Mem 439. This vector 440 is

scrambled by the long and short PN codes **441** to generate the CDMA encoded chip vector $Z(n)$ **442**.

FIG. **6A** depicts a representative implementation block diagram for the Rx fast decoder algorithm in equations **(11)** for the example **58** in equations **(10)** of the multiple data rate generalized Hybrid Walsh CDMA decoding and replaces the real Walsh decoding **27** in FIG. **3A**. Inputs **443** are the Rx estimates $\hat{Z}(n)$ of the Tx CDMA encoded chip vectors $Z(n)$. Long and short PN codes are removed **444** from $\hat{Z}(n)$ to yield the Rx estimate $\hat{Z}_n(n)$ **445** of the Tx Hybrid Walsh encoded chips $Z_n(n)$. The $Z_n(n)$ is decoded by the generalized Hybrid Walsh fast decoding algorithm in equations **(11)** by executing an $M=M_0M_1$ -pass computation starting with the M_0 -pass computation of the Hybrid Walsh decoding **446** and followed by the M_1 -pass computation of the DFT decoding **447** to yield $Z^{(M)}$ which is reordered and rescaled by multiplying by the factor $(1/4N)$ and handed off to the $\hat{Z}(c)$ memory Mem **448** for de-multiplexing (De-Mux) **449** to yield the Rx decoded estimates $\{\hat{Z}(u_{m,k_m})\}$ **450** of the Tx data symbols $\{Z(u_{m,k_m})\}$ **434** in FIG. **5A**.

It should be obvious to anyone skilled in the communications art that the example implementations in FIG. **5A, 6A** clearly define the fundamental CDMA signal processing relevant to this invention disclosure and it is obvious that these examples are representative of the other possible signal processing approaches.